

1 **Brain/MINDS Beyond Human Brain MRI Study: Multi-Site Harmonization for Brain**
2 **Disorders Throughout the Lifespan**

3 Running Head: Brain/MINDS Beyond MRI study

4
5 Shinsuke Koike, M.D., Ph.D.^{1,2,3,4}; Saori C Tanaka, Ph.D.⁵; Tomohisa Okada, M.D., Ph.D.⁶;
6 Toshihiko Aso, M.D., Ph.D.⁷; Michiko Asano, Ph.D.¹; Norihide Maikusa, Ph.D.^{1,8}; Kentaro
7 Morita, M.D., Ph.D.⁹; Naohiro Okada, M.D., Ph.D.^{2,4,10}; Masaki Fukunaga, Ph.D.¹¹; Akiko
8 Uematsu, Ph.D.¹; Hiroki Togo, MSc.⁸; Atsushi Miyazaki, Ph.D.¹²; Katsutoshi Murata, MSc.¹³;
9 Yuta Urushibata, MSc.¹³; Joonas Autio, Ph.D.⁷; Takayuki Ose, MSc.⁷; Junichiro Yoshimoto,
10 Ph.D.⁵; Toshiyuki Araki, M.D., Ph.D.¹⁴; Matthew F Glasser, M.D., Ph.D.^{15,16}; David C Van
11 Essen, Ph.D.¹⁵; Megumi Maruyama, Ph.D.¹⁷; Norihiro Sadato, M.D., Ph.D.¹¹; Mitsuo Kawato,
12 Ph.D.^{5,18}; Kiyoto Kasai, M.D., Ph.D.^{2,3,4,10}; Yasumasa Okamoto, M.D., Ph.D.¹⁹; Takashi
13 Hanakawa, M.D., Ph.D.^{8,20}; Takuya Hayashi, M.D., Ph.D.⁷; Brain/MINDS Beyond Human Brain
14 MRI Group

15
16 1) Center for Evolutionary Cognitive Sciences (ECS), Graduate School of Art and Sciences, The
17 University of Tokyo, Meguro-ku, Tokyo 153-8902, Japan

18 2) University of Tokyo Institute for Diversity & Adaptation of Human Mind (UTIDAHM),
19 Meguro-ku, Tokyo 153-8902, Japan

20 3) University of Tokyo Center for Integrative Science of Human Behavior (CiSHuB), 3-8-1
21 Komaba, Meguro-ku, Tokyo 153-8902, Japan

22 4) The International Research Center for Neurointelligence (WPI-IRCN), Institutes for
23 Advanced Study (UTIAS), University of Tokyo, 7-3-1 Hongo, Bunkyo-ku, Tokyo 113-8654,
24 Japan

25 5) Brain Information Communication Research Laboratory Group, Advanced
26 Telecommunications Research Institutes International (ATR), Kyoto 619-0288, Japan

27 6) Human Brain Research Center, Kyoto University, Kyoto 606-8507, Japan

28 7) Laboratory for Brain Connectomics Imaging, RIKEN Center for Biosystems Dynamics
29 Research, Hyogo 650-0047, Japan

30 8) Integrative Brain Imaging Center, National Center of Neurology and Psychiatry, Kodaira-shi,
31 Tokyo 187-8551, Japan

32 9) Department of Rehabilitation, Graduate School of Medicine, The University of Tokyo,
33 Bunkyo-ku, Tokyo 113-8655, Japan

34 10) Department of Neuropsychiatry, Graduate School of Medicine, The University of Tokyo,
35 Bunkyo-ku, Tokyo 113-8655, Japan

36 11) Division of Cerebral Integration, Department of System Neuroscience, National Institute for
37 Physiological Sciences, Okazaki 444-8585, Japan

38 12) Tamagawa University Brain Science Institute, 6-1-1 Tamagawagakuen, Machida, Tokyo
39 194-8610, Japan

40 13) Siemens Healthcare K.K. Shinagawa-ku, Tokyo 141-8644, Japan

41 14) Department of Peripheral Nervous System Research, National Institute of Neuroscience,
42 National Center of Neurology and Psychiatry, Kodaira, Tokyo 187-8551, Japan

43 15) Department of Neuroscience, Washington University School of Medicine, St Louis, Missouri
44 USA

45 16) Department of Radiology, Washington University School of Medicine, St Louis, Missouri,
46 USA

47 17) Research Enhancement Strategy Office, National Institute for Physiological Sciences,
48 Okazaki 444-8585, Japan

49 18) Center for Advanced Intelligence Project, RIKEN, Tokyo 103-0027, Japan

50 19) Department of Psychiatry and Neurosciences, Hiroshima University, Hiroshima 734-8551,
51 Japan

52 20) Department of Integrated Neuroanatomy and Neuroimaging, Kyoto University Graduate
53 School of Medicine, Kyoto 606-8303, Japan

54

55 **Corresponding to:**

56 Takuya Hayashi, M.D., Ph.D.

57 Laboratory for Brain Connectomics Imaging,

58 RIKEN Center for Biosystems Dynamics Research

59 6-7-3 Minatojima-minami-machi, Chuo-ku, Kobe, Hyogo 650-0047

60 E-mail: takuya.hayashi@riken.jp

61 Tel: +81-78-304-7140

62 Fax: +81-78-304-7141

63 **Abstract**

64 Psychiatric and neurological disorders are afflictions of the brain that can affect individuals
65 throughout their lifespan. Many brain magnetic resonance imaging (MRI) studies have been
66 conducted; however, imaging-based diagnostic and therapeutic biomarkers are not yet well
67 established. The Brain/MINDS Beyond human brain MRI project (FY2018 ~ FY2023) is a
68 multi-site harmonization study aiming to establish clinically-relevant imaging biomarkers using
69 multiple high-performance scanners, standardized multi-modal imaging, and a study design that
70 includes traveling subjects. This project began with 13 clinical research sites that collect MRI
71 data on psychiatric and neurological disorders across the lifespan and three research sites that
72 design and develop measurement procedures, neuroimaging protocols, data storage and sharing,
73 and analysis tools. Brain images obtained with the Harmonization protocol (HARP) are
74 preprocessed and analyzed using approaches developed by the Human Connectome Project,
75 generating preliminary cortical structure, function, and connectivity measures that are
76 comparable across scanners. The use of ‘travelling subjects’, in which study participants travel to
77 multiple sites to undergo scanning with standardized neuroimaging techniques, enable us to
78 minimize the measurement bias between scanners and protocols and to increase the sensitivity
79 and specificity of case-control studies. All the imaging and demographic and clinical data are
80 shared between the participating sites and will be made publicly available in 2024. To the best of
81 our knowledge, this is the first multi-site human brain MRI project to explore multiple
82 psychiatric and neurological disorders across the lifespan. The Brain/MINDS Beyond human
83 brain MRI project will help to identify the common and disease-specific pathophysiology
84 features of brain diseases and develop imaging biomarkers for clinical practice.

85 **Keywords**

86 Multi-site Study; HCP-style Brain Imaging; Psychiatric Disorders; Neurological Disorders;

87 Harmonization Protocol; Traveling Subjects

88 **Text**

89 **Abbreviations**

- 90 DALYs, disability-adjusted life years
- 91 MRI, magnetic resonance imaging
- 92 HCP, Human Connectome Project
- 93 ABCD, Adolescent Brain Cognitive Development
- 94 BPD, bipolar disorder
- 95 MDD, major depressive disorder
- 96 DecNef, Decoded Neurofeedback
- 97 ASD, autism spectrum disorder
- 98 ADNI, Alzheimer's Disease Neuroimaging Initiative
- 99 AD, Alzheimer's disease
- 100 MCI, mild cognitive impairment
- 101 PPMI, Parkinson's Progression Markers Initiative
- 102 PD, Parkinson's disease
- 103 T1w, T1-weighted
- 104 T2w, T2-weighted
- 105 rsfMRI, resting state functional MRI
- 106 CRHD, Connectome Related to Human Disease
- 107 GLM, general linear model
- 108 TS, traveling subject
- 109 AMED, Japan Agency for Medical Research and Development
- 110 Brain/MINDS Beyond, Strategic International Brain Science Research Promotion Program

- 111 HARP, Harmonization protocol
- 112 DWI, diffusion-weighted imaging
- 113 QC, quality control
- 114 MNI, Montreal Neurological Institute
- 115 MSM, multi-modal surface matching
- 116 GLMM, general linear mixed model
- 117 CIFTI, Connectivity Informatics Technology Initiative
- 118 FEF, frontal eye field
- 119 PEF, premotor eye field
- 120 PSL, peri-sylvian language
- 121 STS, superior temporal sulcus
- 122 NODDI, nerite orientation and density imaging

123 **1. Introduction**

124 Psychiatric and neurological disorders are afflictions of the brain that can affect individuals
125 throughout their lifespans. Using the disability-adjusted life years (DALYs), which is a measure
126 of disease burden proposed by the World Health Organization Global Burden of Disease study,
127 in 2010 mental and behavioral disorders accounted for 7.4% of the total DALYs and
128 neurological disorders accounted for 3.0% (Murray et al., 2012), up from 5.4% and 1.9% in
129 1990, respectively. Since the 1990s, technical advances in magnetic resonance imaging (MRI)
130 have allowed detailed analysis of the organization of brain function and structure in humans.
131 Recent high-quality MRI studies with a large cohort are expected to provide neurobiological and
132 life-span information in healthy subjects (Glasser et al., 2016b; Harms et al., 2018; Miller et al.,
133 2016), which will hopefully provide diagnostic utility for patients with psychiatric and
134 neurological disorders (Drysdale et al., 2017; Elliott et al., 2018b; Koutsouleris et al., 2015;
135 Nunes et al., 2018). However, the diagnostic value of brain MRI in psychiatric disorders has not
136 yet been established, presumably because effect sizes tend to be small and overlap with
137 variability in healthy individuals (Yamashita et al., 2019). Protocols of scanning and analysis
138 have rarely been standardized across projects, though that has begun to change - especially for
139 large projects such as the Human Connectome Project (HCP; (Van Essen et al., 2012)), UK
140 Biobank (Miller et al., 2016), and the Adolescent Brain Cognitive Development (ABCD) project
141 (Casey et al., 2018).

142

143 *1.1. Previous multi-site neuroimaging studies for neuropsychiatric disorders*

144 Several brain imaging projects have attempted to identify suitable biomarkers in
145 neuropsychiatric diseases. Recent multi-site neuroimaging mega studies have revealed well-

146 replicated and clinically applicable findings from structural images; the Enhancing
147 NeuroImaging Genetics through Meta-Analysis Consortium in the U.S. (n = 4,568) and the
148 Cognitive Genetics Collaborative Research Organization in Japan (n = 2,564) replicated findings
149 that patients with schizophrenia have volumetric alterations of subcortical structures when
150 compared to healthy controls (Okada et al., 2016; van Erp et al., 2016). The findings were partly
151 evident in other psychiatric disorders, such as bipolar disorder (BPD) and major depressive
152 disorder (MDD) (Hibar et al., 2018; Schmaal et al., 2017; Schmaal et al., 2016; van Erp et al.,
153 2016). Using resting-state functional MRI (rsfMRI), a multi-site study successfully developed
154 generalized classifiers for psychiatric disorders. The Decoded Neurofeedback (DecNef) Project
155 (<https://bicr.atr.jp/decnefpro/>), a multi-site neuroimaging study in Japan (12 sites, n = 2,409),
156 developed a generalized classifier for autism spectrum disorder (ASD) with a high accuracy—
157 not only for the data in three Japanese sites (85%) but also for the Autism Brain Imaging Data
158 Exchange dataset (75%) (Yahata et al., 2016). The project also quantified the spectrum of
159 psychiatric disorders by applying the ASD classifier to other multi-disorder datasets
160 (schizophrenia, MDD, and attention-deficit/hyperactivity disorder). Therefore, the focus of
161 mega-analyses is shifting from features found in case-control studies to cross-disease
162 comparisons that can identify common and disease-specific features.

163 In the field of neurodegenerative disease, the Alzheimer’s Disease Neuroimaging
164 Initiative (ADNI) is one of many major multi-site neuroimaging and biomarker studies of
165 Alzheimer’s disease (AD) and mild cognitive impairment (MCI) that was started in 2005 in
166 North America (Mueller et al., 2005; Weiner et al., 2015). It contributed to the development of
167 blood and imaging biomarkers, the understanding of the biology and pathology of aging, and to
168 date has resulted in over 1,800 publications. ADNI also impacted worldwide ADNI-like

169 programs in many countries including Japan, Australia, Argentina, Taiwan, China, Korea,
170 Europe, and Italy. The Japanese ADNI (J-ADNI) conducted a multi-site neuroimaging study on
171 cognitively normal elderly patients, MCI, and mild AD (n = 537), which emphasized the
172 harmonization of the protocol and procedures with the ADNI (Iwatsubo et al., 2018). J-ADNI
173 also developed machine learning techniques using feature-ranking, a genetic algorithm, and a
174 structural MRI-based atrophy measure to predict the conversion from MCI to AD (Beheshti et
175 al., 2017). Inspired by the Parkinson's Progression Markers Initiative (PPMI; (Parkinson
176 Progression Marker Initiative, 2011), the Japanese (J-) PPMI team has also started a cohort in
177 patients with rapid eye movement sleep behavioral disorder, which is regarded to be prodromal
178 to Parkinson's disease (PD) (Mukai and Murata, 2017).

179 These previous mega-studies have contributed to the discovery of potential mechanisms
180 and biomarkers of multiple brain disorders. However, most of these imaging biomarkers have a
181 relatively small effect sizes and the study results were drawn from multi-site data which are often
182 heterogenous and used now outdated traditional low-resolution data acquisition protocols. In
183 addition, there have been no human brain MRI studies that explore multiple psychiatric and
184 neurological disorders that occur through the lifespan within the same cohort of subjects.

185

186 *1.2. High-quality multi-modal MRI protocols and preprocessing pipelines*

187 The HCP developed a broad approach to improving brain imaging data acquisition,
188 preprocessing, analysis, and sharing (Glasser et al., 2016b). It includes: 1) high-quality multi-
189 modal data acquisition; 2) in a large number of subjects; and 3) high-quality data preprocessing
190 and has proven usefulness of MRI techniques for understanding the detailed organization of a
191 healthy human brain (Elliott et al., 2018a; Glasser et al., 2016a; Smith et al., 2015). The HCP

192 aimed to delineate the brain areas and characterize neural pathways that underlie brain function
193 and behavior in 1,200 healthy young adults (Van Essen et al., 2012). HCP scans were performed
194 by a single MR scanner (a customized 3T Skyra, Siemens Healthcare GmbH, Erlangen,
195 Germany) in a total of 4-hour scan time for high-resolution multi-modal data, which included
196 T1-weighted (T1w) images, T2-weighted (T2w) images, diffusion-weighted images (DWI),
197 rsfMRI, and task fMRI (Glasser et al., 2016b; Glasser et al., 2013). The HCP also developed a
198 set of preprocessing pipelines with improved cross-subject alignment that dramatically improves
199 the spatial localization of brain imaging findings and also increasing statistical sensitivity
200 (Coalson et al., 2018; Glasser et al., 2013; Robinson et al., 2018). For the Lifespan Developing
201 and Aging HCP Projects (HCP-D and HCP-A) the original HCP protocol for healthy young
202 adults was shortened, for children and the elderly (60 to 90 min scan time; (Bookheimer et al.,
203 2019; Harms et al., 2018; Somerville et al., 2018), and for psychiatric and neurological disorders
204 (the Connectomes Related to Human Disease [CRHD];
205 <https://www.humanconnectome.org/disease-studies>), and adolescent development (the ABCD
206 project; (Casey et al., 2018). The UK Biobank used an even more abbreviated scanning approach
207 to collect a much larger number of cohort (n = 100,000) to predict health conditions (Miller et
208 al., 2016).

209 Many of these high-quality multimodal projects have been based on a single or small
210 number of the same model scanners at different sites and thus did not fully address
211 standardization of the data acquisition across different scanner models or vendors. We aim to
212 accelerate harmonization technologies to be used in at least five scanner platforms by combining
213 approaches to high-quality imaging acquisition, preprocessing, study design, and statistical bias
214 correction to potentially improve the sensitivity and validity of imaging biomarkers.

215

216 *1.3. Traveling subjects*

217 A harmonization approach is required for individual-based statistics using a multi-site dataset,
218 even when the brain images are obtained using the same machine and protocol, because the data
219 from each site has the bias from hardware and scanning protocol (measurement bias) and
220 sampling variability (i.e. age, sex, handedness, and socioeconomic status). If measurement biases
221 were correlated or anti-correlated with a specific disease state this would result in a positive or
222 negative bias in a given measure, whereas uncorrelated biases would merely reduce sensitivity
223 (i.e. SNR) of the measure. Sampling biases due to biological differences in the sampled
224 populations should also be considered for both case and control groups. Data harmonization has
225 been proposed to control for these biases, including a general linear model (GLM) with the site
226 as the covariate, a Bayesian approach (Fortin et al., 2018; Fortin et al., 2017), and a meta-
227 analytic approach (Okada et al., 2016; van Erp et al., 2016), but the methods used for controlling
228 both biases are unable to distinguish between them (Yamashita et al., 2019). Inter-site cross-
229 validation by machine learning and deep learning techniques is a method that aims to remove
230 bias without any specific preparation if large-sample datasets are available (Nunes et al., 2018).
231 However, this method extracts stable characteristics across the images and is limited to using
232 only a part of the information for further analysis. In addition, it is unclear whether the classifiers
233 obtained by such methods can be applied to an independent new site of the initial multi-site
234 project.

235 The traveling subject (TS) approach is a powerful research design to control for site
236 differences (Figure 1). This approach requires the images from the same participants at all the
237 participating sites, but also requires significant effort from the sites and the participants when

238 compared to other harmonization methods listed above, and the TS scans must be completed
239 before the analysis starts. However, the TS approach can differentiate most of the sample
240 variability from measurement bias (Yamashita et al., 2019). The DecNef Project explored
241 rsfMRI functional connectivity for multiple psychiatric diseases and scanned nine TS
242 participants who received repeated MRI measurements at all sites. Measurement and sampling
243 biases for each group (schizophrenia, MDD, ASD, and healthy controls) were segregated from
244 individual and disease-specific factors as the rest of sampling variability. The results showed that
245 the effects of both bias types on functional connectivity were greater than or equal to those of
246 disease-specific factors. With regard to measurement bias, differences in phase encoding
247 direction had the biggest effect size when compared to those of vendor, coil, and scanner within
248 the same vendor. The harmonization method was estimated to reduce measurement bias by 29%
249 and improve the signal-to-noise ratio by 40% (Yamashita et al., 2019). Further investigations are
250 needed to determine the best approach for reducing sampling bias arising from biological
251 differences in the sampled population.

252

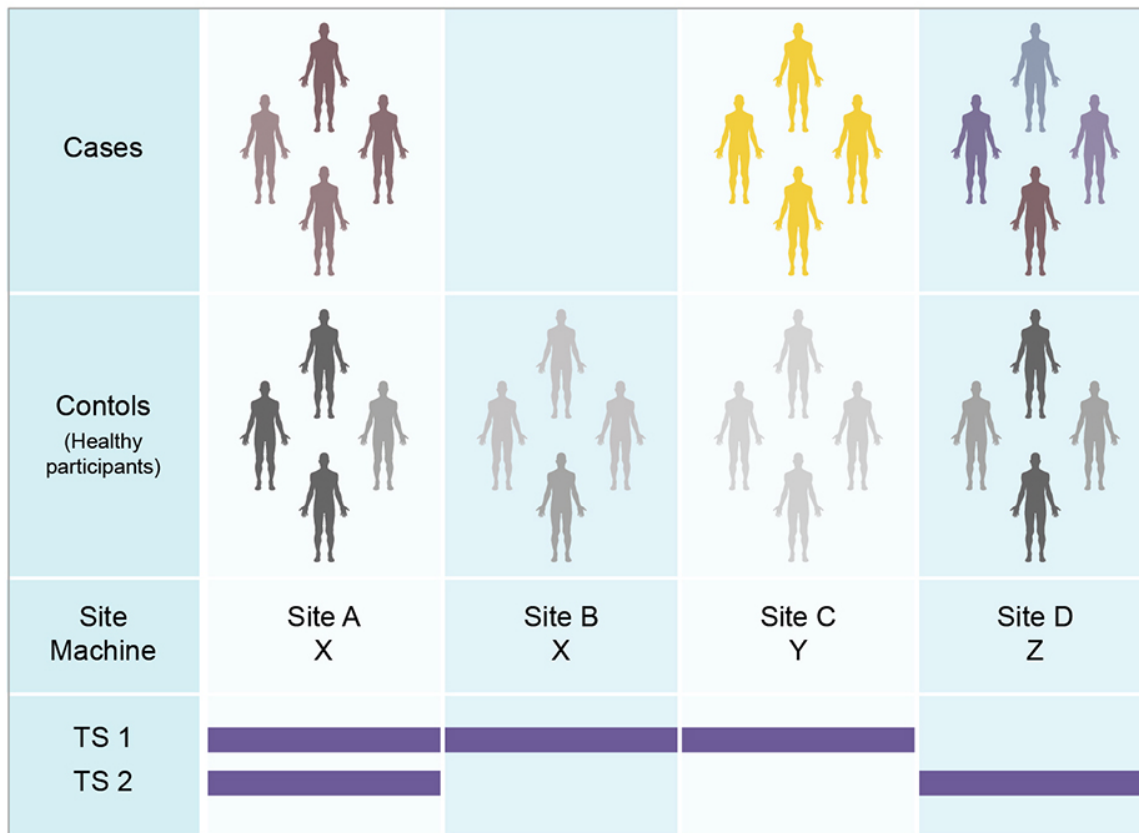


Figure 1. Case-control studies and traveling subject approach.

(Top) When we analyze multi-site data from a set of case-control MRI studies, we must consider machine and protocol-derived bias (measurement bias) as well as sampling bias (from biological differences in the sampled populations). Even if the machine and protocol are the same between sites (e.g. Sites A and B), measurement bias may still occur because of slight differences in the magnetic or radiofrequency fields, etc. Sampling bias should be considered for patient groups as well as control groups, given that the control participants were recruited according to the demographics in the patient group. (Bottom) The traveling subject (TS) harmonization approach enables us to combine with case-control datasets by differentiating between measurement and sampling biases (Yamashita et al., 2019). Based on the general linear model (GLM), TS participants need to receive measurements from all participating sites (e.g. only TS 1 dataset). To reduce the effort of TS participants and participating sites, this project applies a general linear mixed model (GLMM) approach and hub-and-spoke model to the TS project. With this approach, all participants receive scans at one or more hub sites (site A), and measurement bias is calculated using multiple TS datasets by means of a GLMM (TS 1 and 2).

253

254 1.4. Brain/MINDS Beyond project

255 The Strategic International Brain Science Research Promotion Program (Brain/MINDS Beyond;
256 FY2018–FY2023; <https://brainminds-beyond.jp/>) was funded by the Japan Agency for Medical
257 Research and Development (AMED) to support global brain research by enhancing collaboration
258 with the domestic projects of other countries. Brain/MINDS Beyond consists of four research
259 groups: G1-1, Identification of the pathogenic mechanism of psychiatric and neurological
260 disorders through the acquisition and analysis of brain MRI-scan images and clinical data
261 (Developmental [G1-1D], adult [G1-1A], and senescent [G1-1S] stages); G1-2, Brain MRI data
262 acquisition, analysis, and informatics; G2, Research involving an inter-species comparison of
263 human and nonhuman primate brains by structural and functional parcellation and homology
264 analyses; and G3, Development and application of technologies, such as neuro-feedback through
265 collaboration with artificial intelligence research projects as well as the Innovative Research
266 Group. In human brain imaging, G1-1 intends to measure human participants, including patients
267 with neuropsychiatric disorders, across the lifespan, and G1-2 intends to coordinate and support
268 data acquisition, storage, preprocessing, analysis, and distribution (Figure 2 and Table 1). The
269 Brain/MINDS Beyond MRI working group also set up a standardized procedure for MRI data
270 acquisition (Harmonization protocol [HARP]) and clinical and neurocognitive data assessment
271 (Tables 2 and 3). Following previous multi-site studies in Japan (Iwatsubo et al., 2018; Okada et
272 al., 2016; Yahata et al., 2016; Yamashita et al., 2019), the overall goal is to find an altered brain
273 imaging characteristics in psychiatric and neurological disorders that can be applied to future
274 therapeutic investigations and clinical devices. To address limitations of previous findings in
275 multi-site studies, we are using high performance research-based MRI scanners and we modeled
276 our multi-modal protocol (T1w images, T2w images, diffusion-weighted imaging [DWI],
277 rsfMRI, task fMRI, quantitative susceptibility mapping, and arterial spin labeling) on that used

278 by the HCP and ABCD study projects. We are also obtaining a TS dataset for the harmonization
279 of the clinical MRI datasets and the development of technical tools to harmonize the multi-site
280 data. Once the project period ends, the data will be openly distributed to researchers via a public
281 database.

282 Here, we introduce the Brain/MINDS Beyond human brain MRI project and show
283 preliminary results in high-quality neuroimaging using the TS data that is amenable to
284 harmonization. We then discuss our plans for investigating the neural basis of psychiatric and
285 neurological disorders in the hope of developing therapeutic targets and devices that are
286 applicable to clinical settings.

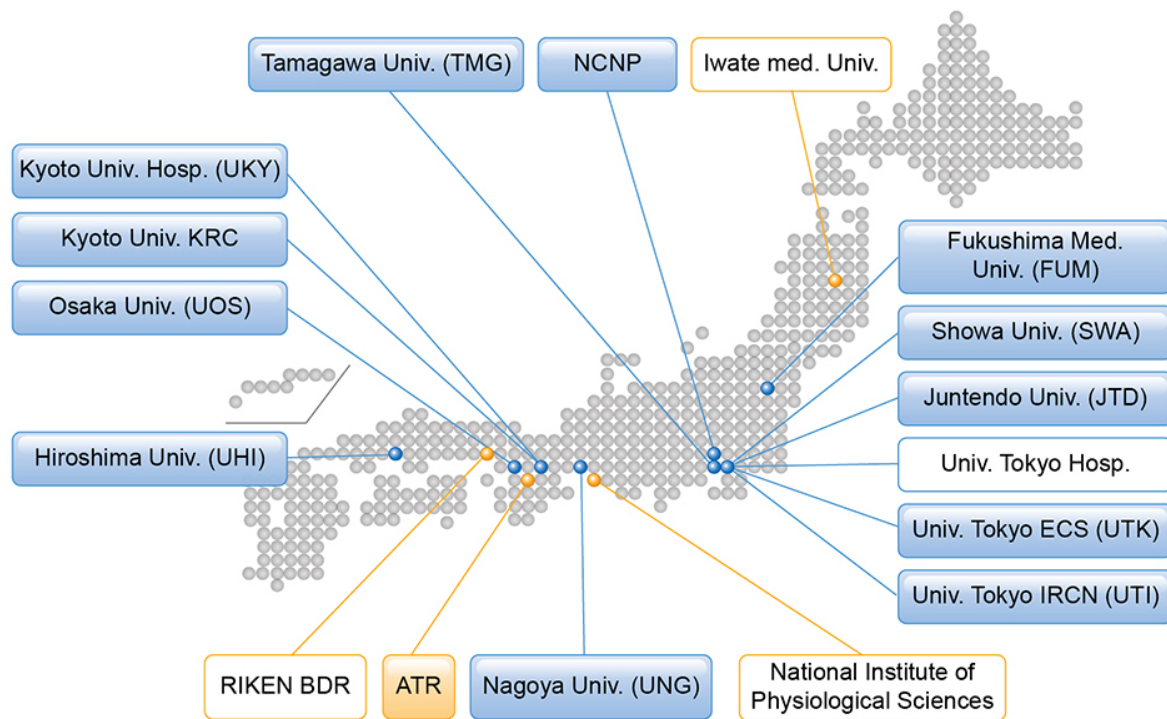


Figure 2. Brain/MINDS Beyond human brain MRI project.

Institutes in the blue boxes show measurement and analysis sites for neuropsychiatric disorders, and those in the orange boxes show analysis support sites. Institutes listed in boxes with a colored background represent participation in the traveling subject project.

287

288 **2. Brain/MINDS Beyond human brain MRI study**

289 *2.1. Participating sites and target population*

290 As of March 2020, 13 sites have approved this study project, received approval from their
291 respective ethical review board(s), and obtained clinical and TS measurements using the
292 appropriate MRI scanners (Table 1). Of these, 5 sites mainly explore psychiatric disorders
293 (schizophrenia, ASD, MDD, and BPD), 4 sites neurological disorders (AD, PD, multiple system
294 atrophy, progressive supranuclear palsy, chronic pain disorder, and epilepsy), and 2 sites both
295 categories. Two sites measure the general adolescent population to investigate brain development
296 and recruit through advertisement and cohort studies (Ando et al., 2019; Okada et al., 2019).
297 Each site intends to obtain brain images and demographic (and clinical) characteristics for
298 clinical cases and match controls for age, sex, premorbid IQ or educational attainment, socio-
299 economic status, and handedness (See Cognitive and behavioral assessment section). The
300 exclusion criteria were set by each study purpose (i.e. low premorbid IQ, history of loss of
301 consciousness for more than 5 min, illegal drug use, and alcohol dependency). Illegal drug use
302 can be a major concern for disease onset and poor prognosis, especially for psychiatric disorders.
303 However, there is far less illegal drug use in Japan compared to Western European countries
304 (Degenhardt et al., 2008; Lee and Kwon, 2016), and most of the participating sites excluded
305 those with a current illegal drug use or previous history of regular use (Koike et al., 2013).

306 For the TS project, 75 healthy adults planned to undergo 6 to 8 scans at three or more
307 sites within 6 months (See Traveling Subject Project section). Five or more participants per site
308 were recruited. Each participant received test-retest scans at the recruitment site and underwent
309 scans at different sites including a hub site. We set up three hub sites, according to a hub-and-

310 spoke model, in which all participants received scans using a MAGNETOM Prisma scanner
 311 (Siemens Healthcare GmbH, Erlangen, Germany) and the CRHD and HARP protocols.

312 **Table 1. Participating sites of the Brain/MINDS Beyond MRI project.**

Site	Research group	Role	MRI scanner (System version)	Protocol	Main target population
UTK	G1-1D, G1-2	Data acquisition/Analysis	Prisma (VE11C)	CRHD	Adolescent cohort, HP, ASD, Sch, MDD, Epilepsy
UTI	G1-1D, G1-2	Data acquisition/Sharing	Prisma (VE11C)	CRHD	HP, ASD, Sch, MDD, BPD
ATR	G1-2, G3	Data acquisition/Sharing/Analysis	Prisma (VE11C)	CRHD	HP
FUM	G1-1S	Data acquisition	Skyra (VE11C)	HARP	HP, AD, PD
TMG	G1-1D	HARP setup/Data acquisition	Trio (VB19A)	HARP	Adolescent cohort
SWA	G1-1D, G3, IR	HARP setup/Data acquisition	Skyra (VE11E)	HARP	HP, ASD
NCNP	G1-1S	HARP setup/Data acquisition/Sharing/Analysis	Verio Tim+Dot (VD13A)	HARP	HP, Sch, MDD, AD, PD
JTD	IR	Data acquisition	Prisma (VE11C)	HARP	HP, Chronic pain
UOS	G2	Data acquisition	Prisma (VE11C)	HARP	HP, PD, MSA, PSP
UHI	G1-1A, G3	HARP setup/Data acquisition	Skyra (VE11C)	HARP	HP, MDD, BPD
UNG	BM	Data acquisition	Verio (VB17A)	HARP	HP, Sch
UKY	G1-1S	HARP setup/Data acquisition	Skyra (VE11C)	HARP	HP, AD, PD
KRC	G1-1A	Data acquisition	Verio (VB17A)	HARP	HP, Sch, MDD, BPD
BDR	G1-2	HARP setup/Data Analysis	Prisma (VE11C)	HARP	NA

313 Abbreviations: UTK, The University of Tokyo ECS (Komaba Campus); UTI, The University of
 314 Tokyo IRCN; FUM, Fukushima Medical University; TMG, Tamagawa Academy & University;
 315 SWA, Showa University; NCNP, National Center of Neurology and Psychiatry; JTD, Juntendo
 316 Hospital; ATR, Advanced Telecommunications Research Institute International; UOS, Osaka
 317 University; UHI, Hiroshima University; UNG, Nagoya University; UKY, Kyoto University;
 318 KRC, Kyoto University Kokoro Research Center; BDR, RIKEN Center for Biosystems
 319 Dynamics Research; IR, Innovative Research Group in Brain/MINDS Beyond; BM,
 320 Brain/MINDS project; CRHD, Human Connectome Studies Related To Human Disease protocol;
 321 HARP, harmonization protocol; HP, healthy participants; ASD, autism spectrum disorders; Sch,
 322 schizophrenia; MDD, major depressive disorder; BPD, bipolar disorder; AD, Alzheimer's
 323 disease; PD, Parkinson disease; MSA, multiple system atrophy; PSP, progressive supranuclear
 324 palsy.
 325

326 *2.2. Harmonized brain MRI protocols*

327 We developed protocols that minimize potential differences related to measurement and increase
328 the MR image sensitivity to brain organization in psychiatric and neurological disorders. From a
329 neurobiological perspective, the cerebral cortex is organized by a 2D sheet-like structure with an
330 average thickness of 2.6 mm embedded and folded in the ~1300 mL of brain volume (Glasser et
331 al., 2016b). From a neuroimaging perspective, the spatial resolution and homogeneity of the
332 images are important factors that may induce bias and error during the image analysis; these
333 include partial voluming, image distortion, errors in brain segmentation, and registration. Of
334 these, respecting spatial fidelity of neuroanatomical structures is the most important approach for
335 achieving unbiased imaging (Glasser et al., 2016b). Therefore, the spatial resolution of the
336 imaging was determined based on cortical thickness and was matched across all scanners. The
337 phase encoding direction of EPI-based functional and diffusion MRI is an important factor that
338 relates to spatial distortion (and signal loss in fMRI) in association with the polarity of the
339 direction, echo spacing, and B0 magnetic field homogeneity; therefore, we acquire a spin-echo
340 filed map with opposing phase encoding directions to enable distortion correction (Andersson et
341 al., 2003). Based on these strategies, two MRI protocols were planned for use in the project: 1) a
342 harmonized MRI protocol (HARP), which can be run on the multiple MRI scanners/sites within
343 a period of 22 to 65 min; and 2) an ‘HCP style’ MRI protocol used by HCP CRHD for the high-
344 performance 3T MRI scanner (e.g. MAGNETOM Prisma).

345 The HARP was created to be used at multiple MRI scanners/sites, and it was designed to
346 obtain high-quality and standardized brain MRI data in a ‘clinically’ practical window of time
347 (Table 2 and Supplementary Table S1). The parameters of the MRI scanners were as follows: 1)
348 static magnetic field strength of 3T; 2) multi-array head coil with 32 or more channels; and 3)
349 ability to perform a multi-band EPI sequence provided from Center for Magnetic Resonance

350 Research, University of Minnesota with an acceleration factor of 6 (Moeller et al., 2010;
351 Setsompop et al., 2012; Xu et al., 2013). In 2019, the protocol was adapted for use with five MRI
352 scanners/systems (MAGNETOM Prisma, Skyra, Trio A Tim, Verio, and Verio Dot; Siemens
353 Healthcare GmbH, Erlangen, Germany), and we plan to expand it to different MRI
354 scanners/vendors during the project period. The HARP was intended to perform the brain scan
355 within a period of ~ 30 min using a high-resolution structural MRI scan (T1w and T2w, spatial
356 resolution of 0.8 mm) and two high-sensitive rsfMRI scans with opposing phase directions, a
357 spatial resolution of 2.4 mm, and a temporal resolution of 0.8 s for a total of 10 minutes. The
358 protocols also include optional sequences for four additional rsfMRI scans, task fMRI (Emotion
359 and CARIT) (Winter and Sheridan, 2014), two DWI scans with opposing phase encoding
360 directions, quantitative susceptibility mapping, and arterial spin labeling. The minimum and
361 maximum scanning time of the HARP is 22 and 65 min, respectively (Table 2). The preliminary
362 results across scanners and multi-array coils in the same subject (ID = 9503) revealed that the
363 temporal signal-to-noise ratio (tSNR) was very high in all the scanners. The mean \pm standard
364 deviation across 32k greyordinates was 161 ± 80 in the Prisma at UTK, 155 ± 81 in the Verio
365 Dot at SWA, 151 ± 72 in the Skyra fit at SWA, 151 ± 80 in the Verio at ATR, and 150 ± 74 in
366 the Prisma fit at ATR; the values and their distributions were similar across scanners/sites
367 (Figure 3A).

368 The CRHD protocol was planned for collaboration with the HCP CRHD for the Early
369 Psychosis Project. The HCP CRHD protocol also included high-resolution structural MRI
370 (spatial resolution of 0.8 mm), high-resolution resting-state fMRI (spatial resolution of 2 mm)
371 with an opposing phase encoding direction and longer scan time, and high-resolution and high
372 angular diffusion MRI.

373 The installation of the protocols in the MRI scanners was ensured by conducting
374 hierarchical parameter checks and site visits at the beginning of the measurement period. After
375 the protocol installation, each site sent XML files of the installed protocol from the MRI scanner
376 to the protocol management site (UTK), and all the parameters were confirmed with a checksum
377 algorithm using R (R Core Team, 2018). This process was useful for validating the protocols
378 across sites/scanners because some of the MRI scanners actually underwent inappropriate
379 installation and were set with different parameters. The results were then sent back to the
380 collaborators, who edited the parameters. We also checked the DICOM files that are deposited in
381 the ATR XNAT server. In this phase, we checked the parameters, slice numbers, and diffusion
382 gradient information (bvec and bval).

383 The manuals were shared and used at the sites for protocol installation, demographic and
384 clinical assessment before the scan (e.g. handedness), and the assessment of and instruction to
385 participants during the scan (e.g. general instruction during the scan, fixation to the cross during
386 rsfMRI scans, and the assessment of sleepiness during the rsfMRI).

387 **Table 2. CRHD and HARP protocols.**

Subset	Sequence	Duration		Participant instruction
		Prisma	Skyra, Trio, Verio Dot, Verio HARP	
		CRHD	HARP	
rsfMRI 1	SEF AP	0:32	0:06	Fixation
	BOLD AP	5:46	5:08	Fixation
	SEF PA	0:32	0:06	Fixation
	BOLD PA	5:46	5:08	Fixation
Structure	T1 MPR	6:38	5:22	Rest
	T2 SPC	5:57	5:31	5:22-6:26 Rest
Subtotal		25 min	22 min	22-23 min
ASL		NA	2:45 ^b	Rest
QSM		NA	5:03 ^c	Rest
DWI	AP	6:07	3:29	4:50 Rest
	PA	6:05	3:32	4:54 Rest
	AP	5:39	NA	NA Rest
	PA	5:39	NA	NA Rest
rsfMRI 2	See rsfMRI 1 ^a	13 min	11 min	Fixation
rsfMRI 3	See rsfMRI 1 ^a	NA	11 min	Fixation
Task fMRI EMOTION	SEF AP	NA	0.06	Task
	SEF PA	NA	0.06	Task
	BOLD PA	NA	4.08	Task
Task fMRI CARIT	SEF AP	NA	0.06	Task
	SEF PA	NA	0.06	Task
	BOLD PA	NA	4.08	Task
Total		61 min	68 min	59-68 min

388 Abbreviations: rsfMRI, resting-state functional MRI; ASL, arterial spin labeling; QSM,
 389 quantitative susceptibility mapping; DWI, diffusion weighted imaging; SEF, spin echo field
 390 mapping; BOLD, blood oxygenation level dependent; T1 MPR, T1-weighted magnetization
 391 prepared rapid acquisition with gradient echo; T2 SPC, T2-weighted sampling perfection with
 392 application optimized contrasts using different flip angle evolutions.

393 a A set of SEF AP, BOLD AP, SEF PA, and BOLD PA.

394 b Only for Prisma and Skyra.

395 c Only for Prisma, Skyra, and Verio Dot.

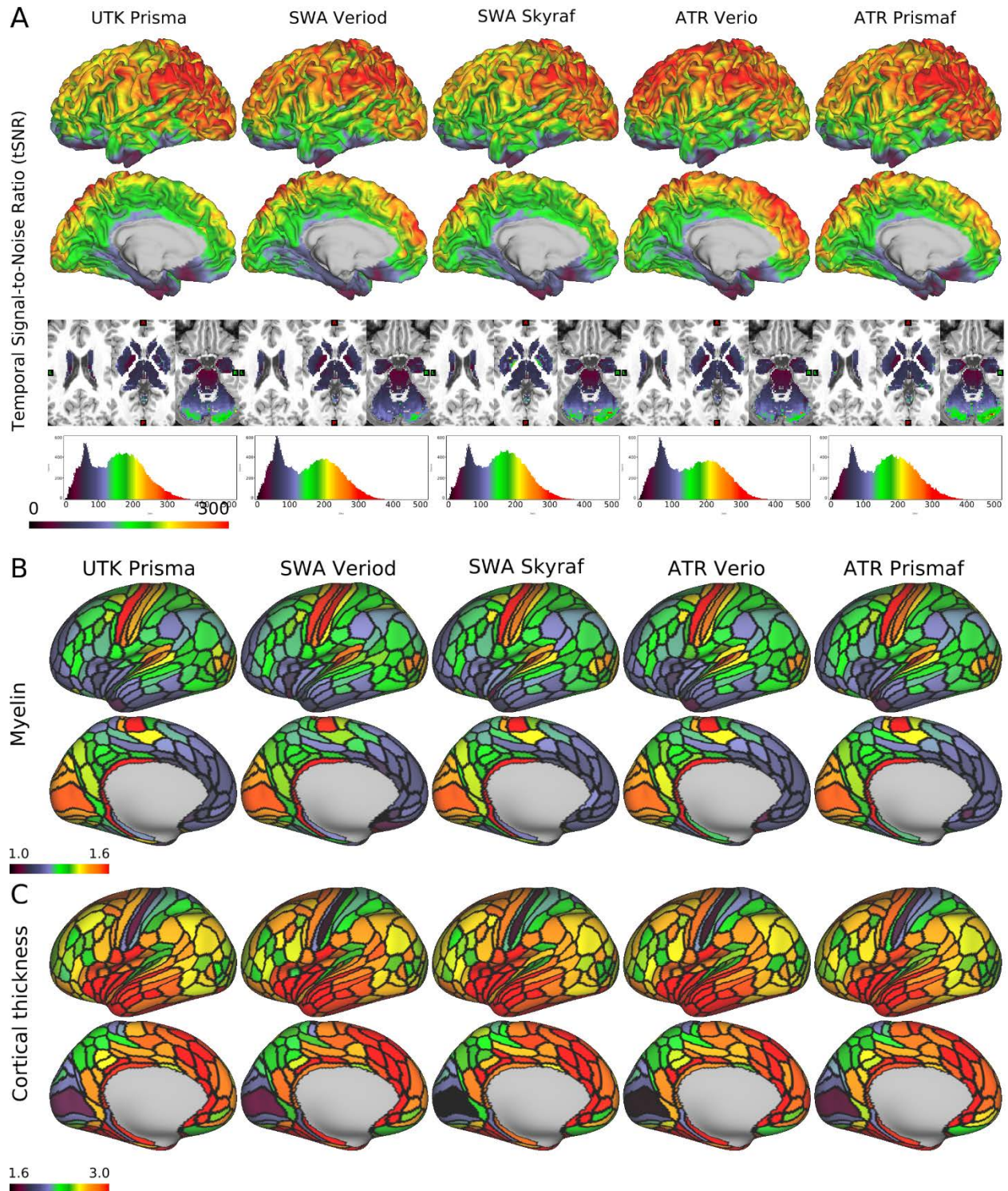


Figure 3. Quality of MRI and preliminary cortical structures obtained by HARP in a single traveling subject across scanners/sites.

A) Temporal signal-to-noise ratio (tSNR) obtained in a single subject (ID = 9503) across different scanners/sites by a harmonized MRI protocol (a sequence of functional MRI in HARP using a multi-band echo planar imaging with TR/TE = 800/34.4 ms; see Supplementary Table S1 for other details). The images from top to bottom show color-coded tSNR maps in 32k greyordinates (see main text) overlaid on the lateral and medial surface of the mid-thickness surface of the left hemisphere, the subcortical sections of the T1w image, and the histogram of the tSNR values. B) Cortical myelin contrast (T1w/T2w ratio) across different scanners. The myelin contrast is corrected for the biasfield and parcellated by the HCP MMP v1.0 (Glasser et al., 2016a). C) The map shows cortical thickness across different scanners. Cortical thickness is corrected by curvature and parcellated by the HCP MMP v1.0. The tSNR, myelin map and cortical thickness are comparable across scanners. Data at <https://balsa.wustl.edu/7q4P9> and <https://balsa.wustl.edu/6Vvqv>

396

397 *2.3. Cognitive and behavioral assessment*

398 Each participating site assesses demographic characteristics (i.e. age, sex, and socioeconomic
399 status), clinical characteristics (i.e. diagnosis, symptom severity, cognitive function, and general
400 functioning), and subjective social evaluations (i.e. quality of life and well-being) (Table 3).

401 Each subgroup (G1-1D, G1-1A, G1-1S, and G1-2 TS) indicates standard scales, some of which
402 are uniform across subgroups and easier to share and use when analyzing brain images.

403 **Table 3. Clinical and neuropsychological assessment.**

	G1-1D	G1-1A	G1-1S
Depression	K6 or BDI-II	BDI-II and PHQ-9	PHQ-9 and BDI-II/GDS-15
Anxiety	—	GAD-7	STAI
Autism	AQ-10, AQ-50 or SRS-2 (for developmental disorders)	AQ-10 or AQ-50	—
Psychosis	APSS	—	NPI-Q
Intellectual ability	JART-25 or WAIS-III (WISC at the age of 15 years or less) Information and Picture completion subtests	JART-25	JART-25
Cognitive function	CANTAB or BACS-J	CANTAB or BACS-J	ADAS-Cog11, CDT, CDR, FAB, HVLT-R, JLO, MMSE, MoCA-J, SDMT, TMT-A/B, WMS-R
General function and disability	GAF, mGAF or WHO-DAS 2.0	GAF, mGAF or WHO-DAS 2.0	Schwab & England ADL
Quality of life	EQ-5D	EQ-5D	PASE
Well-being	WHO-5	WHO-5	SHAPS
Handedness	EHR5 or UTokyo	EHR5 or UTokyo	UTokyo

404 Abbreviations: K6, 6-item Kessler Screening Scale for Psychological Distress; BDI-II, Beck
405 Depression Inventory – Second Edition; PHQ-9, Patient Health Questionnaire-9; GDS-15,
406 Geriatric Depression Scale 15; GAD-7, General Anxiety Disorder-7; STAI, State-Trait Anxiety
407 Inventory; AQ-10, 10-item short version of the Autism Spectrum Quotient; AQ-50, Autism
408 Spectrum Quotient (original version); APSS, Adolescent Psychotic-like Symptom Screener;
409 NPI-Q, Neuro Psychiatric Inventory-Brief Questionnaire Form; JART-25, 25-item short version
410 of the Japanese Adult Reading Test; WAIS-III, Wechsler Adult Intelligence Scale – Third
411 Edition; GAF, Global Assessment of Functioning; mGAF, modified GAF; WHO-DAS 2.0, the
412 World Health Organization Disability Assessment Schedule II; Schwab & England ADL,
413 Modified Schwab and England ADL (Activities of Daily Living) scale; CANTAB, Cambridge
414 Neuropsychological Test Automated Battery; BACS-J, the Brief Assessment of Cognition in
415 Schizophrenia Japanese version; ADAS-Cog, Alzheimer’s Disease Assessment Scale-cognitive
416 component; CDT, Clock Drawing Test; CDR, Clinical Dementia Rating; FAB, Frontal
417 Assessment Battery; HVLT-R, Hopkins Verbal Learning Test-Revised; JLO, Judgment of Line
418 Orientation; MMSE, Mini-Mental State Examination; MoCA-J, Japanese version of Montreal
419 Cognitive Assessment; SDMT, Symbol Digit Modality Test; TMT-A/B, Trail Making Test Parts
420 A and B; WMS-R, Wechsler Memory Scale-Revised; EQ-5D, EuroQol 5 Dimension
421 questionnaire; WHO-5, World Health Organization-Five Well-Being Index; PASE, Physical
422 Activity Scale for Elderly; SHAPS, Snaith-Hamilton Pleasure Scale; EHI, Edinburgh
423 Handedness Inventory; UTokyo, 14-item Rating Scale of Handedness for Biological Psychiatry
424 Research among Japanese People.

425 *2.4. Travelling subject project*

426 Based on the previous study (Yamashita et al., 2019), we also conducted a TS project for the
427 CRHD and HARP protocols. In some sites, we also use the former protocols to combine with
428 existing large-scale datasets (Iwatsubo et al., 2018; Okada et al., 2016; Yahata et al., 2016;
429 Yamashita et al., 2019). Because we limit the scanners, head coils, and protocols in this project,
430 we expect to see reduced measurement biases, which may enhance the disease-related effect size
431 in clinical studies and provide better ways to diminish bias in future studies.

432 The previous data harmonization using the TS dataset was based on a GLM (Yamashita
433 et al., 2019); however, the present TS project may provide a harmonization method using a
434 general linear mixed model (GLMM; Figure 1), given that the new protocols require a longer
435 scan time compared to previous protocols (~20 min for T1w imaging and rsfMRI). To ensure the
436 images from all sites are well harmonized, we applied a hub-and-spoke model to arrange
437 traveling scans at each recruitment site (Supplementary Table S2). Each participant undergoes
438 CRHD and HARP scans using the Prisma (~2 hours) at one or more hub sites (UTK, UTI, and
439 ATR) to harmonize the data within the Brain/MINDS Beyond project and other projects (e.g.
440 Brain/MINDS, HCP, and ABCD) and test the difference in quality between the protocols. The
441 other visiting sites were determined in consideration of the site locations, machine differences,
442 and project similarities between the sites. Each participant receives multiple scans at the
443 recruitment site to assess the test-retest reliability (1 hour x 2 sessions). The interval between
444 scans may vary by site due to scanner time restrictions but we aim to determine whether the gap
445 between test-retest scans would be associated with reliability.

446 For the TS project, 75 healthy adults—five or more participants per site—are scheduled
447 to undergo 6 to 8 scans at three or more sites within 6 months (Supplementary Table S2). The

448 total number of scans and spokes between the sites are expected to be 455 and 465, respectively
449 (Figure 4A). As of March 2020, 74 participants were registered and 405 scans (89.0 %) were
450 completed and uploaded to the ATR XNAT server. The data provided 368 spokes (76.1 %,
451 Figure 4B). The TS project will end in August 2020.

452 We also plan another TS project including task fMRI sequences in HARP to see the
453 validity and reliability of the task fMRI paradigms and the applicability of harmonizing higher
454 quality registration using the task fMRI data. The task fMRI TS study is set to begin September
455 2020 and will include 10 participants, 4 sites (UTK [including test-retest], UTI, TMG and SWA),
456 and a total of 50 scans.

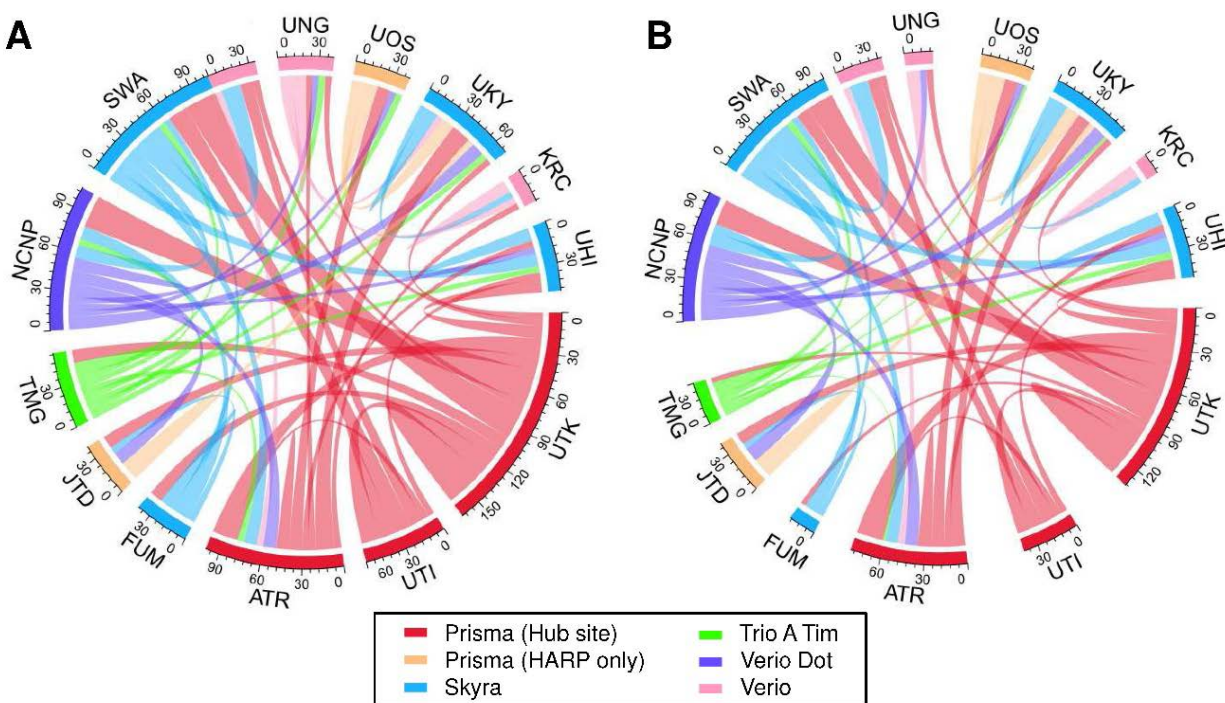


Figure 4. Expected and current data connection of the traveling subjects.

Data connections in the traveling subject project that were (A) initially planned and (B) the actual connections as of March 2020. Hub sites using Prisma and other sites using Prisma, Skyra, Trio A Tim, Verio Dot, and Verio are illustrated in red, orange, blue, green, purple, and pink, respectively.

457

458 *2.5. Data storage, preprocessing, and quality control*

459 *2.5.1. Data logistics*

460 Brain MR images obtained using the CRHD and HARP protocols in this study project and
461 related studies are stored, preprocessed, and distributed using the XNAT server system
462 (<https://www.xnat.org/>) (Figure 5). Due to the legacy of previous multi-site studies (Iwatsubo et
463 al., 2018; Yahata et al., 2016; Yamashita et al., 2019), several data centers were already available
464 for this project. The images obtained from the development and adult projects (G1-1D and G1-
465 1A) will be sent to an XNAT server at ATR and the clinical data will be sent to UTI. For the
466 senescent project (G1-1S), all the data will be sent to the NCNP (Iwatsubo et al., 2018). The TS
467 data will also be sent to the ATR server shown in dashed lines. When uploading to the XNAT
468 server, personal information (i.e. name and date of birth) contained in DICOM is automatically
469 removed using an anonymization script of XNAT. A defacing procedure is performed for T1w
470 and T2w images. These processes de-identify the MRI data. After manually checking whether
471 the face images are completely obscured, all the anonymized MRI data are shared using Amazon
472 AWS with RIKEN BDR, in which all image preprocessing is performed (See Preprocessing
473 pipelines section). Preprocessed data are sent back to the servers and can be seen with limited
474 access (i.e. participating sites). After a quality control (QC), cleaned imaging data with a
475 demographic and clinical datasheet will be stored in the distribution server(s). All data will be
476 also sent to backup server(s).

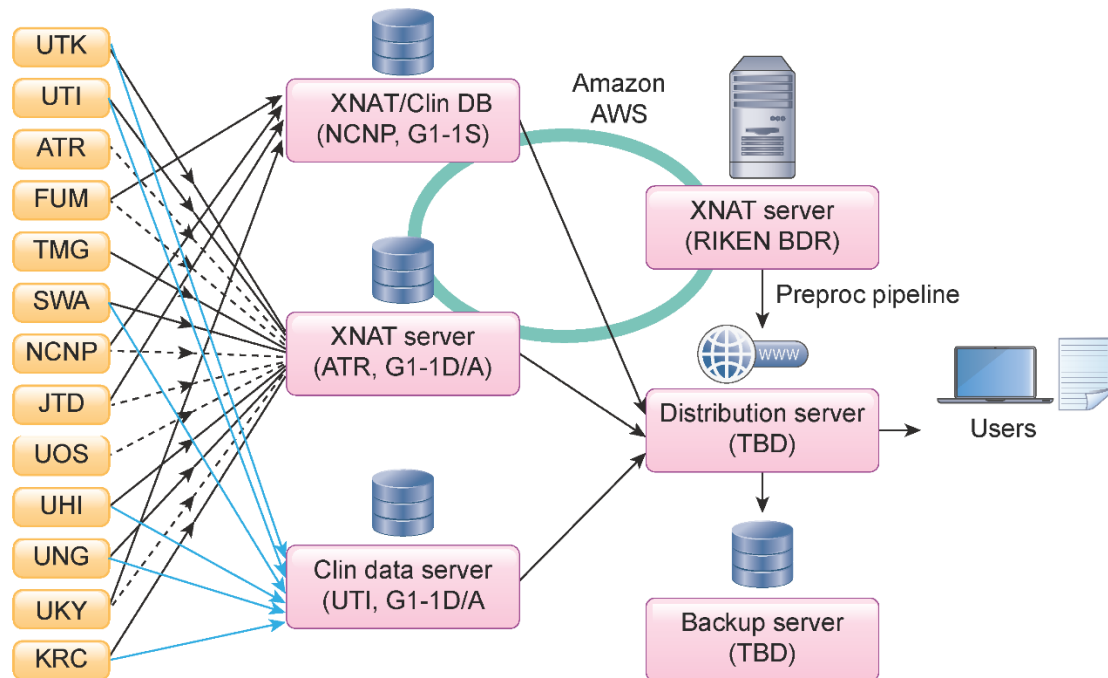


Figure 5. Data storage, preprocessing, quality check, and data sharing.

MRI (black line) and clinical (blue line) data from G1-1D and G1-1A sites are sent to the XNAT server and a data server at ATR and UTI, respectively. All data from G1-1S sites are sent to an XNAT server and a data server managed by NCNP, as this group applied a standard clinical assessment protocol to the project following a previous multi-site study. Traveling subject data from G1-1S sites are also sent to the XNAT server in ATR (dot line). XNAT servers at NCNP, ATR, and RIKEN BDR are linked by Amazon AWS to share the imaging data. NCNP manages a separate server for storing clinical data (Clin DB) being collected from the participants in this project. All MR images are preprocessed at RIKEN BDR. All MR images are preprocessed at RIKEN BDR. All of the raw and preprocessed data will be stored and provided to the users in a distribution server. A backup server will be placed at a different site.

477

478 2.5.2. Preprocessing pipelines

479 All neuroimaging data are preprocessed at RIKEN BDR for this project. The MR images are sent

480 via Amazon S3 to a high-throughput parallel computing system at RIKEN BDR for

481 preprocessing. The preprocessing is performed using the HCP pipeline 4.2.0 (Glasser et al.,

482 2013) with modifications for adapting and harmonizing multiple scanners. In brief, the structural

483 MRI (T1w and T2w) is first corrected for image distortions related to the gradient nonlinearity in

484 each scanner type and the inhomogeneity of the B0 static magnetic field in each scan. The signal

485 homogeneity is dealt with by prescan normalization and is also improved by a biasfield
486 correction using T1w and T2w images (Glasser and Van Essen, 2011). The T1w and T2w
487 images are fed into non-linear registration to the Montreal Neurological Institute (MNI) space
488 and used for cortical surface reconstruction using FreeSurfer (Fischl, 2012), surface registration
489 using multi-modal surface matching (MSM) (Robinson et al., 2018) and folding pattern
490 (MSMsulc); this is followed by the creation of a myelin map using T1w divided by T2w and
491 surface mapping (Glasser and Van Essen, 2011). An example of a cortical myelin map in a single
492 subject (ID = 9503) across scanners/sites is parcellated by HCP MMP v1.0 (Glasser et al., 2016a)
493 and presented in Figure 3B, revealing the typical cortical distribution of the high myelin contrast
494 in the primary sensorimotor (areas 1, 3a, 3b, 4), auditory (A1), visual (V1), middle temporal, and
495 ventral prefrontal (47m) areas—as demonstrated previously (Glasser and Van Essen, 2011), and
496 is quite comparable between scanners.

497 The functional MRI data is corrected for distortion (gradient nonlinearity and B0-
498 inhomogeneity) and motion. The distortion from B0 static field inhomogeneity is corrected by
499 means of opposite phase encoding spin echo fieldmap data using TOPUP (Andersson et al.,
500 2003); it is then warped and resampled to MNI space at a 2 mm resolution and saved as a volume
501 in the Neuroimaging Informatics Technology Initiative (NIFTI) format. The region of the
502 cortical ribbon in the fMRI volume is further mapped onto the cortical surface and combined
503 with voxels in the subcortical gray region to create 32k greyordinates in the Connectivity
504 Informatics Technology Initiative (CIFTI) format. Multiple runs of the fMRI data are merged
505 and fed into independent component analyses (ICA) followed by an automated classification of
506 noise components and the removal of noise components using FIX (Salimi-Khorshidi et al.,
507 2014) (Glasser et al., 2018). The automated classifier is trained using the data in this project and

508 its accuracy is maximized. The denoised fMRI data, in combination with other cortical metrics
509 (myelin, thickness; Figure 3B and 3C, respectively), is further used for multi-modal registrations
510 (MSMAll) over the cortical surface, followed by ‘de-drifting’ (removing registration bias after
511 multimodal registration) based on the group sampled in this study (Glasser et al., 2016a). The
512 resting-state seed-based functional connectivity in an example of a single subject (ID = 9503)
513 revealed a typical pattern over the cerebral cortex across scanners/sites; the left frontal eye field
514 (FEF)-seed functional connectivity showed symmetric coactivation in the bilateral premotor eye
515 field (PEF) (Figure 6A), whereas the left area 55b-seed FC showed an asymmetric language
516 network distributed in the peri-sylvian language (PSL) area, superior temporal sulcus (STS), and
517 areas 44/45 predominantly in the left hemisphere (Figure 6B).

518 The diffusion MRI is corrected for distortion and motion due to gradient nonlinearity,
519 eddy current, motion, and B0 static field inhomogeneity using EDDY (Andersson and
520 Sotiropoulos, 2016). The signal dropouts, susceptibility artefact, and their interaction with
521 motion were also corrected (Andersson et al., 2018; Andersson et al., 2017). The resulting
522 diffusion volumes are merged into a single volume and resampled in the subject’s real physical
523 space aligned according to the ACPC convention. Diffusion modeling is performed using nerite
524 orientation density imaging (NODDI) (Fukutomi et al., 2018; Zhang et al., 2012), and a Bayesian
525 estimation of crossing fibers (Behrens et al., 2003; Sotiropoulos et al., 2016). Diffusion
526 probabilistic tractography (Behrens et al., 2003) is also performed in a surface-based analysis
527 (Donahue et al., 2016).

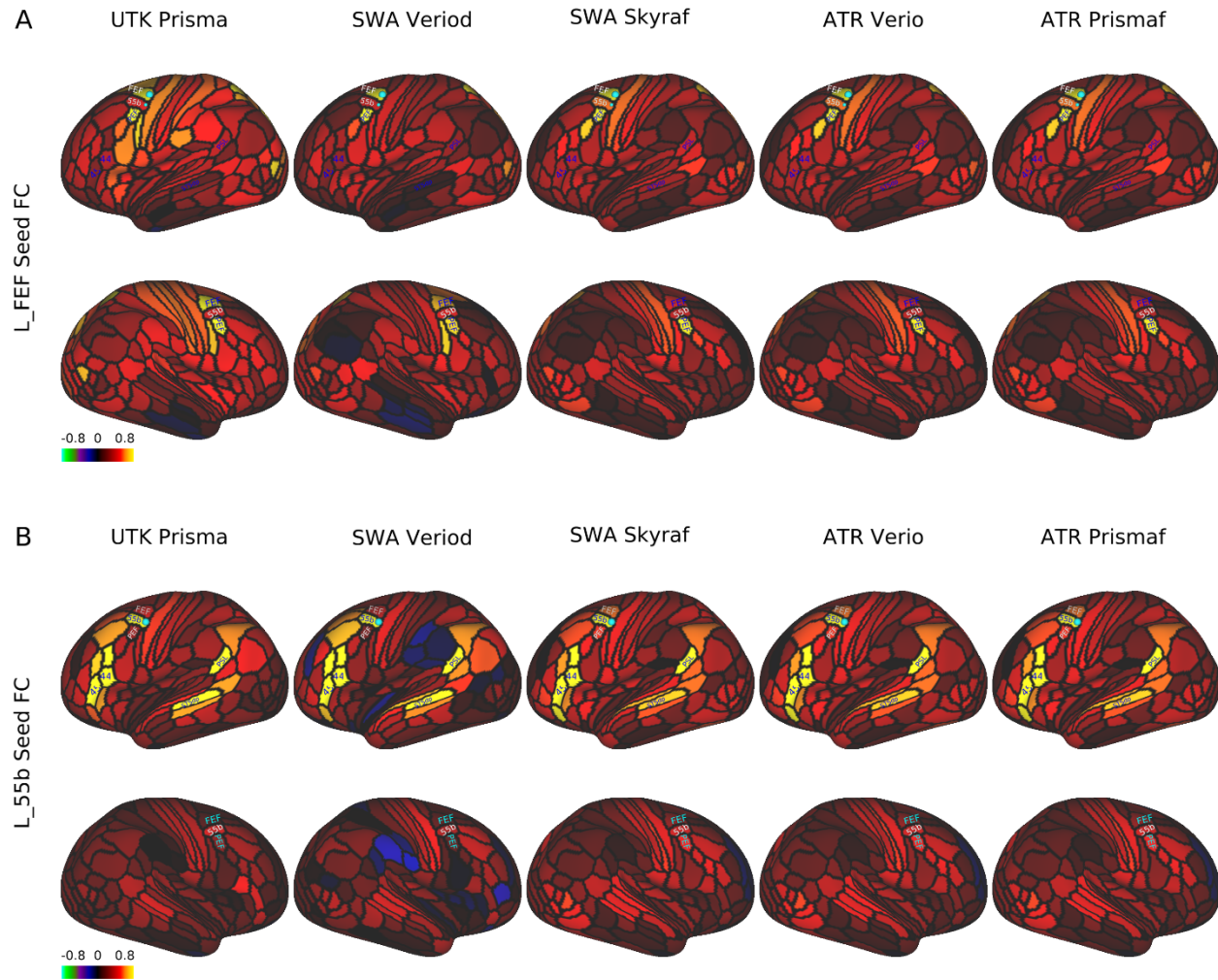


Figure 6. Seed-based resting-state functional connectivity in a single traveling subject across scanners/sites

In a single subject (ID = 9503), the resting-state fMRI scans (5 min x 4) were collected using a scanning protocol of HARP across different scanners/sites (see Supplementary Table S1), preprocessed, and denoised by a surface-based analysis to generate parcellated functional connectivity (FC) using the HCP MMP v1.0 (Glasser et al., 2016a). A) FC seeded from the left frontal eye field (FEF), which was distributed symmetrically in the bilateral premotor eye field (PEF) and comparable across scanners/sites. B) FC seeded from the left area 55b, which showed an asymmetric language network predominant in the left hemisphere that was comparable across scanners/sites. The language network is distributed in the areas of 44/45, superior temporal sulcus, dorsal posterior part (STSdp), and peri-sylvian language (PSL). Data at <https://balsa.wustl.edu/1B9VG> and <https://balsa.wustl.edu/5Xr71>

528

529 *2.5.3 Preliminary travelling subject data*

530 Here, we show the preliminary results obtained from the initial TS data (as detailed in section
531 2.4). In the initial TS study, five healthy subjects participated and travelled across five sites and
532 received MRI scanning with HARP in different scanners, and four of them completed all the
533 travelling scans as planned. Datasets were analyzed with the current version of preprocessing
534 (see section 2.5.2) and each of the cortical thickness, myelin, and resting-state functional
535 connectivity was parcellated using HCP MMP v1.0 (Glasser et al., 2016a) as described above (a
536 part of the parcellated data in an exemplar subject [ID = 9503] was already shown in Figure 3
537 and 6). To investigate similarity of the data, each of the parcellated metrics was fed into an
538 analysis of Spearman's rank correlation across subjects and sites/scanners. Figure 7 shows the
539 resultant similarity matrices which demonstrate higher correlation coefficients of within-subjects
540 than those of cross-subjects in all the metrics of cortical thickness, myelin, and functional
541 connectivity. These findings suggest that our approach with harmonized protocols and
542 preprocessing is promising for capturing a subject-specific imaging biomarker.

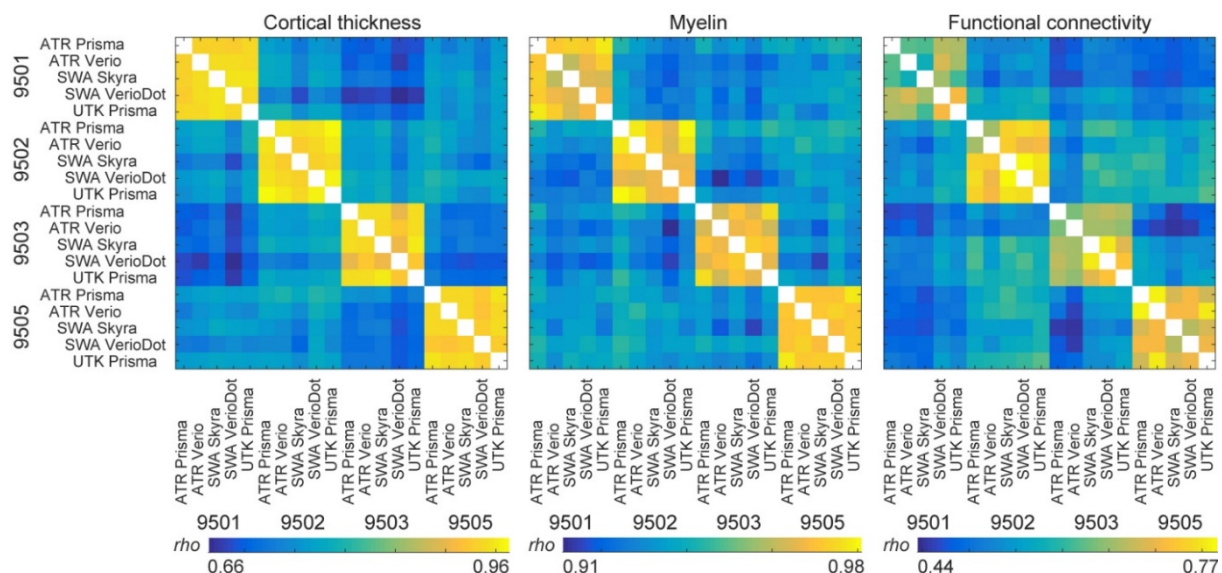


Figure 7. Similarity of the cortical metrics across subjects and sites/scanners in preliminary travelling subject study

From left to right show the correlation matrices of the parcellated cortical thickness, myelin and functional connectivity in four travelling subjects (TS). Number of parcellated metrics

used for analysis were 360 for thickness and myelin and 129,240 for functional connectivity, which cover all the cerebral cortex in both hemispheres. The correlation coefficient of Spearman's rho is presented by a color bar placed at the bottom.

543

544 *2.5.4. Quality control*

545 QC is implemented in several stages: 1) a brief image check during each scan; 2) an anomaly and
546 abnormality inspection by the radiologists; 3) an assessment of raw data image quality when
547 uploading data to the XNAT server; and 4) preprocessed image quality checks. QC 1 is
548 conducted by site personnel and the participants are rescanned within the same session if scan
549 time remains, if the images have major artifacts, such as those due to head movement. QC 2 is
550 conducted by radiologists at the measurement site or other sites if any radiologist at the site is
551 unable to check the images. QC 3 is manually conducted by researchers at the measurement sites
552 before uploading the data to a server for all images in reference to the HCP QC manual (Marcus
553 et al., 2013). After uploading the images to the XNAT servers, all images are first checked
554 according to the DICOM file information as to whether the images are correctly updated. The
555 researchers at each site are informed of missing DICOM files and any irregular parameters
556 detected in the DICOM files. In QC 3, the T1w and T2w images are manually checked as to
557 whether the face images are completely removed. Then, signal distributions of the myelin map
558 are checked for outliers because of its sensitivity to several artifacts and errors such as motion,
559 reconstruction of the images, and cortical surface reconstruction. Functional and diffusion
560 images are automatically checked for outliers, and the images and data will be checked by visual
561 inspection. In the QC 3 process, a QC pipeline will be implemented for checking the images
562 (Marcus et al., 2013). QC 4 uses preprocessed CIFTI images that will be checked in several
563 preprocessing steps. Any irregular scans and remarks are recorded in the clinical data servers and
564 the information will be used when determining the eligibility criteria for each study.

565

566 *2.6. Ethical regulation*

567 Sharing neuropsychiatric patient data, which may contain information linked to subjects’
568 privacy, requires special attention (Sadato et al., 2019). Therefore, the Brain/MINDS Beyond
569 project put NCNP as the core site for supporting ethical considerations. Before participating in
570 the project, all institutions are required to receive approval from their ethical review board
571 regarding their research plans. This includes the following points and ethical documentation: 1)
572 MR images and clinical data of the participants may be shared within the Brain/MINDS Beyond
573 project or Japanese/International scientific institutions for collaboration. De-identified MR
574 images with limited clinical data (see below) may become publicly accessible on an open
575 database for research purposes. 2) MR images of the participants may be compared with non-
576 human primate MRI data. 3) Intellectual property rights originating from the research of the
577 Brain/MINDS Beyond project shall be attributed to the institutes of the researchers and not the
578 participants. All participants must provide written informed consent to participate in this project
579 after receiving a complete explanation of the experiment.

580 The Japanese regulations for the sharing of personal information used for research
581 purposes requires attention in dealing with two types of data: “individual identification codes”
582 and “special care-required personal information”
583 (<http://www.japaneselawtranslation.go.jp/law/detail/?id=2781&vm=04&re=01>). Individual
584 identification codes are direct identifiers—information sufficient to identify a specific individual.
585 Special care-required personal information represents indirect identifiers needing special care in
586 handling so as not to cause potential disadvantages to participants. In consideration of these
587 regulations, data accompanied with the MR images are limited in the publicly accessible open

588 database, and only include 5-year age bins, sex, diagnostic information, handedness, simple
589 socioeconomic status, clinical scale scores, and sleepiness scale scores. In the Brain/MINDS
590 Beyond project, we exclude the datasets of MR images containing facial information from the
591 data in the publicly accessible open database.

592

593 *2.7. Data sharing*

594 In the current provisional plan of sharing the collected data, we have designated three types of
595 data sharing:

596 1) Access via an open database: de-identified MR images and limited clinical data are to become
597 publicly accessible for research purposes after the research period ends. The initial release will
598 be scheduled in 2024. Basic demographic and clinical characteristics such as 5-year age bin, sex,
599 socioeconomic status, (premorbid) estimated intellectual quotient, main diagnosis, representative
600 scale scores for each disease and sleepiness during rsfMRI scan will be shared.

601 2) Application-based sharing: MR images and the clinical datasets are shared after receiving
602 application approval for data usage by the Brain/MINDS Beyond human brain MRI study
603 working group. Applicants are required to obtain approval of their research plan from the ethical
604 review board of their institution and request the dataset type in the application form. The
605 working group discusses the eligibility of the applicants, as well as the availability of the
606 requested dataset, the ethical consideration in the Brain/MINDS Beyond site(s), and any conflict
607 from other applications. Data is released from the distribution server of the Brain/MINDS
608 Beyond project with limited access.

609 3) Collaboration-based sharing: This form of sharing is used for individual collaborative studies.
610 A research proposal collaborating with the institute(s) in the Brain/MINDS Beyond project is

611 approved by the ethical review board of the institute(s). Data is shared from the relevant
612 institute(s).

613 **3. Discussion**

614 The Brain/MINDS Beyond human brain MRI study expands upon research from previous multi-
615 site neuroimaging studies in Japan and provides high quality brain images by standardizing
616 multiple MRI scanners and protocols. An unbiased and quantitative assessment of cortical
617 structure and function may be needed for sensitive and specific predictions of any dynamics,
618 perturbations, or disorders of the brain system. Multi-modal cross-disease image datasets are
619 systematically and properly acquired, analyzed, and shared to enable investigation of common
620 and disease-specific features for psychiatric and neurological disorders with a high sensitivity
621 and specificity. A distinct feature of this project is to include a study design with the TS project,
622 which enables harmonizing the multi-site data from lower (i.e. preprocessing) to higher levels
623 (i.e. statistics). The harmonization protocols are available at <http://mriportal.umin.jp>. The
624 Brain/MINDS Beyond human brain MRI project can provide brain imaging biomarkers that are
625 applicable to therapeutic targets and diagnostic supports.

626 To date, several national projects have applied high-quality multimodal MRI protocols, in
627 addition to a preprocessing pipeline, to a large cohort (e.g., HCP, UK biobank, and ABCD).
628 Unlike these multi-site projects, we plan to investigate brain organization associated with brain
629 disorders that occur throughout the lifespan and to develop imaging biomarkers that can be
630 implemented in clinical trials. To facilitate the collection of a larger number of patients with
631 different brain disorders, multiple clinical research sites are participating in this project and
632 cooperating for standardized data acquisitions. The core of the project began from establishing a
633 standardized protocol (i.e. HARP) based on five 3T MRI scanners, but it will continue to develop
634 a comparable protocol for other types of scanners/vendors. The protocol is designed not only for
635 high-resolution structural MRI and high-quality resting-state fMRI, but also for diffusion MRI

636 and other imaging—including scans for correcting distortions. The preprocessing is performed
637 with a surface-based multi-modal analysis to minimize bias largely generated from the variability
638 in cortical folding across subjects (Coalson et al., 2018; Glasser et al., 2016b). The preliminary
639 data demonstrated high quality MRI images and the fidelity of structural and functional brain
640 organizations across scanners/sites. The signal-to-noise ratio of MRI images was very high
641 across scanners/sites (Figure 3A). The cortical metrics of structure (myelin map, thickness)
642 (Figure 3B-C) were comparable to those previously reported in the literature (Fischl and Dale,
643 2000; Glasser and Van Essen, 2011), as well as the functional connectivity related to eye
644 movements involving FEF and PEF (Figure 6A) (Amiez and Petrides, 2009) and a language
645 network involving left 55b, 44/45, STS, and PSL (Figure 6B) (Glasser et al., 2016a). These
646 findings suggest that a surface-based parcellated analysis may provide useful and reliable metrics
647 concerning cortical structure, function, and connectivity, and may potentially contribute to the
648 establishment of multi-modal imaging biomarkers of brain disorders. The initial trial with four
649 TS also demonstrated sensitivity to the subject-specific features across scanners/sites (Figure 7),
650 suggesting the reliability of our harmonizing protocols and preprocessing.

651 The TS approach is a novel harmonization method for multi-site brain image data
652 (Yamashita et al., 2019), which has proven that measurement bias from MRI equipment and
653 protocols can be differentiated from sampling bias between sites. Instead of using a previously
654 applied GLM, we plan to expand the statistical approach to a GLMM in this project. One of the
655 obstacles of the GLMM approach is that it requires a larger number of total scans compared to
656 those in a GLM approach; overlapping scans at hub sites are required for all TS participants to
657 ensure the data connectivity; additionally, a larger number of TS participants is required in the
658 TS project because the degree of freedom can be reduced in the GLMM. However, one of the

659 benefits of the GLMM approach includes that it is flexible with the variability in data
660 acquisition—such as the number of scans per participant and length of scan time per protocol;
661 thus, is suitable for a big project. Furthermore, this approach allows the addition of another site,
662 scanner, and protocol to an existing TS network, which can deal with the future upgrades of
663 scanners and protocols. In fact, the scanners at two sites (UHI and SWA) were upgraded to a
664 MAGNETOM Skyra fit (Siemens Healthcare GmbH, Erlangen, Germany) for institutional
665 reasons after the Brain/MINDS Beyond project had started. Therefore, we customized the TS for
666 two sites to ensure that the data are properly connected before and after the upgrades. Also, the
667 project welcomes other sites to participate in the TS network.

668 Because this project focuses on various brain disorders across the lifespan, we aim to
669 identify common and disease-specific features of psychiatric and neurological disorders. While
670 some case-control studies suggest possible neural mechanisms in a psychiatric disease, other
671 studies suggest that the effects may not be specific to a single entity but instead may be shared
672 across multiple neuropsychiatric disorders (Hibar et al., 2018; Schmaal et al., 2017; Schmaal et
673 al., 2016; van Erp et al., 2016). Such non-specificity may be at least partly addressed by
674 investigating diseases across the lifespan, since some of brain changes reported in psychiatric
675 disorders also occur in aging or development in healthy subjects, e.g. volumetric changes in
676 subcortical structures in schizophrenia (Okada et al., 2016; van Erp et al., 2016) and in healthy
677 aging (O'Shea et al., 2016; Wang et al., 2019). We initially coordinated with 13 sites to explore
678 various psychiatric and neurological disorders throughout the lifespan and to make use of a
679 powerful harmonization method. Therefore, this project aims to identify both the common and
680 disease-specific pathophysiology features of psychiatric and neurological disorders, which will

681 hopefully lead to imaging biomarkers for general clinical practice and the development of
682 candidate therapeutic targets for future clinical trials.

683 In conclusion, the Brain/MINDS Beyond human brain MRI project began with the
684 participation of 13 clinical research sites—all of which have setup brain image scans using the
685 standard MRI scanners and protocols, conducted TS scans, and will share acquired data with the
686 project and the public in the future, and commit to the analysis and publication of the data. To
687 the best of our knowledge, this is the first human brain MRI project to explore psychiatric and
688 neurological disorders across the lifespan. The project aims to discover robust findings which
689 may be directly related to the common or disease-specific pathophysiology features of such
690 diseases and facilitate the development of candidate biomarkers for clinical application and drug
691 discovery.

692 **Acknowledgment**

693 This research was supported by the Agency for Medical Research and Development (AMED)
694 under Grant Numbers JP20dm0307001 (K.K.), JP20dm0307002 (Y.O.), JP20dm0307003
695 (T.Han.), JP20dm0307004 (K.K.), JP20dm0307008 (M.K.), JP20dm`0307020 (N.S.),
696 JP20dm0207069 (S.K.) and JP20dm0307006 (T.Hay.). This study was also supported by the
697 University of Tokyo Center for Integrative Science of Human Behaviour (CiSHuB) and the
698 International Research Center for Neurointelligence (WPI-IRCN) at the University of Tokyo
699 Institutes for Advanced Study (UTIAS).

700

701 **Author Contributions**

702 Shinsuke Koike, Conceptualization, Project administration, Funding acquisition, Writing –
703 original draft, Software, Resources;
704 Saori C Tanaka, Conceptualization, Project administration, Data Curation, Software, Resources,
705 Writing – original draft;
706 Tomohisa Okada, Methodology, Investigation;
707 Toshihiko Aso, Investigation, Formal Analysis, Validation;
708 Michiko Asano, Investigation, Data curation;
709 Norihide Maikusa, Methodology, Resources;
710 Kentaro Morita, Writing – original draft;
711 Naohiro Okada, Investigation, Writing – original draft;
712 Masaki Fukunaga, Methodology;
713 Akiko Uematsu, Methodology, Investigation;
714 Hiroki Togo, Methodology, Investigation;

- 715 Atsushi Miyazaki, Methodology, Investigation;
- 716 Katsutoshi Murata, Methodology;
- 717 Yuta Urushibata, Methodology;
- 718 Joonas Autio, Methodology;
- 719 Takayuki Ose, Methodology;
- 720 Junichiro Yoshimoto, Methodology;
- 721 Toshiyuki Araki, Writing – original draft;
- 722 Matthew F Glasser, Software, Writing - reviewing and editing;
- 723 David C Van Essen, Writing – reviewing and editing;
- 724 Megumi Maruyama, Project administration;
- 725 Norihiro Sadato, Investigation, Funding acquisition, Project administration;
- 726 Mitsuo Kawato, Conceptualization, Funding acquisition, Project administration;
- 727 Kiyoto Kasai, Investigation, Funding acquisition, Project administration, Supervision;
- 728 Yasumasa Okamoto, Investigation, Funding acquisition;
- 729 Takashi Hanakawa, Project administration, Funding Acquisition, Methodology, Investigation,
- 730 Resources, Writing – original draft;
- 731 Takuya Hayashi, Conceptualization, Project administration, Funding Acquisition, Software,
- 732 Resources, Formal Analysis, Writing - original draft, reviewing and editing.
- 733
- 734 **Conflict of interest**
- 735 Katsutoshi Murata and Yuta Urushibara are employed by Siemens Healthcare K.K., Tokyo,
- 736 Japan. The other authors report no financial relationships with commercial interests.
- 737

738 **Data availability**

739 The data presented in Figure 3 and 6 are available at BALSAs

740 (<https://balsa.wustl.edu/study/show/npD26>). Harmonization protocols and other information of the

741 project are available at the BrainMINDS beyond MRI portal site

742 (<http://mriportal.umin.jp/?lang=en>). See also Data sharing section in details of data obtained in

743 future in this project. For proposal and requests for the data usage, please contact to Saori Tanaka

744 (xsaori@atr.jp).

745 **References**

- 746 Amiez, C., Petrides, M., 2009. Anatomical organization of the eye fields in the human and non-human
747 primate frontal cortex. *Prog Neurobiol* 89, 220-230.
- 748 Andersson, J.L., Skare, S., Ashburner, J., 2003. How to correct susceptibility distortions in spin-echo
749 echo-planar images: application to diffusion tensor imaging. *Neuroimage* 20, 870-888.
- 750 Andersson, J.L.R., Graham, M.S., Drobnyak, I., Zhang, H., Campbell, J., 2018. Susceptibility-induced
751 distortion that varies due to motion: Correction in diffusion MR without acquiring additional data.
752 *Neuroimage* 171, 277-295.
- 753 Andersson, J.L.R., Graham, M.S., Drobnyak, I., Zhang, H., Filippini, N., Bastiani, M., 2017. Towards a
754 comprehensive framework for movement and distortion correction of diffusion MR images: Within
755 volume movement. *Neuroimage* 152, 450-466.
- 756 Andersson, J.L.R., Sotiropoulos, S.N., 2016. An integrated approach to correction for off-resonance
757 effects and subject movement in diffusion MR imaging. *Neuroimage* 125, 1063-1078.
- 758 Ando, S., Nishida, A., Yamasaki, S., Koike, S., Morimoto, Y., Hoshino, A., Kanata, S., Fujikawa, S.,
759 Endo, K., Usami, S., Furukawa, T.A., Hiraiwa-Hasegawa, M., Kasai, K., Scientific, T.T.C., Data
760 Collection, T., 2019. Cohort Profile: The Tokyo Teen Cohort study (TTC). *Int J Epidemiol* 48, 1414-
761 1414g.
- 762 Beheshti, I., Maikusa, N., Daneshmand, M., Matsuda, H., Demirel, H., Anbarjafari, G., Japanese-
763 Alzheimer's Disease Neuroimaging, I., 2017. Classification of Alzheimer's Disease and Prediction of
764 Mild Cognitive Impairment Conversion Using Histogram-Based Analysis of Patient-Specific
765 Anatomical Brain Connectivity Networks. *J Alzheimers Dis* 60, 295-304.
- 766 Behrens, T.E., Woolrich, M.W., Jenkinson, M., Johansen-Berg, H., Nunes, R.G., Clare, S., Matthews,
767 P.M., Brady, J.M., Smith, S.M., 2003. Characterization and propagation of uncertainty in diffusion-
768 weighted MR imaging. *Magn Reson Med* 50, 1077-1088.
- 769 Bookheimer, S.Y., Salat, D.H., Terpstra, M., Ances, B.M., Barch, D.M., Buckner, R.L., Burgess, G.C.,
770 Curtiss, S.W., Diaz-Santos, M., Elam, J.S., Fischl, B., Greve, D.N., Hagy, H.A., Harms, M.P., Hatch,
771 O.M., Hedden, T., Hodge, C., Japardi, K.C., Kuhn, T.P., Ly, T.K., Smith, S.M., Somerville, L.H.,
772 Ugurbil, K., van der Kouwe, A., Van Essen, D., Woods, R.P., Yacoub, E., 2019. The Lifespan Human
773 Connectome Project in Aging: An overview. *Neuroimage* 185, 335-348.
- 774 Casey, B.J., Cannonier, T., Conley, M.I., Cohen, A.O., Barch, D.M., Heitzeg, M.M., Soules, M.E.,
775 Teslovich, T., Dellarco, D.V., Garavan, H., Orr, C.A., Wager, T.D., Banich, M.T., Speer, N.K.,
776 Sutherland, M.T., Riedel, M.C., Dick, A.S., Bjork, J.M., Thomas, K.M., Chaarani, B., Mejia, M.H.,
777 Hagler, D.J., Jr., Daniela Cornejo, M., Sicut, C.S., Harms, M.P., Dosenbach, N.U.F., Rosenberg, M.,
778 Earl, E., Bartsch, H., Watts, R., Polimeni, J.R., Kuperman, J.M., Fair, D.A., Dale, A.M., Workgroup,
779 A.I.A., 2018. The Adolescent Brain Cognitive Development (ABCD) study: Imaging acquisition
780 across 21 sites. *Dev Cogn Neurosci* 32, 43-54.
- 781 Coalson, T.S., Van Essen, D.C., Glasser, M.F., 2018. The impact of traditional neuroimaging methods on
782 the spatial localization of cortical areas. *Proc Natl Acad Sci U S A* 115, E6356-E6365.
- 783 Degenhardt, L., Chiu, W.T., Sampson, N., Kessler, R.C., Anthony, J.C., Angermeyer, M., Bruffaerts, R.,
784 de Girolamo, G., Gureje, O., Huang, Y., Karam, A., Kostyuchenko, S., Lepine, J.P., Mora, M.E.,
785 Neumark, Y., Ormel, J.H., Pinto-Meza, A., Posada-Villa, J., Stein, D.J., Takeshima, T., Wells, J.E.,
786 2008. Toward a global view of alcohol, tobacco, cannabis, and cocaine use: findings from the WHO
787 World Mental Health Surveys. *PLoS Med* 5, e141.
- 788 Donahue, C.J., Sotiropoulos, S.N., Jbabdi, S., Hernandez-Fernandez, M., Behrens, T.E., Dyrby, T.B.,
789 Coalson, T., Kennedy, H., Knoblauch, K., Van Essen, D.C., Glasser, M.F., 2016. Using Diffusion
790 Tractography to Predict Cortical Connection Strength and Distance: A Quantitative Comparison with
791 Tracers in the Monkey. *J Neurosci* 36, 6758-6770.
- 792 Drysdale, A.T., Grosenick, L., Downar, J., Dunlop, K., Mansouri, F., Meng, Y., Fetcho, R.N., Zebley, B.,
793 Oathes, D.J., Etkin, A., Schatzberg, A.F., Sudheimer, K., Keller, J., Mayberg, H.S., Gunning, F.M.,
794 Alexopoulos, G.S., Fox, M.D., Pascual-Leone, A., Voss, H.U., Casey, B.J., Dubin, M.J., Liston, C.,

795 2017. Resting-state connectivity biomarkers define neurophysiological subtypes of depression. *Nat*
796 *Med* 23, 28-38.

797 Elliott, L.T., Sharp, K., Alfaro-Almagro, F., Shi, S., Miller, K.L., Douaud, G., Marchini, J., Smith, S.M.,
798 2018a. Genome-wide association studies of brain imaging phenotypes in UK Biobank. *Nature* 562,
799 210-216.

800 Elliott, M.L., Romer, A., Knodt, A.R., Hariri, A.R., 2018b. A Connectome-wide Functional Signature of
801 Transdiagnostic Risk for Mental Illness. *Biol Psychiatry* 84, 452-459.

802 Fischl, B., 2012. FreeSurfer. *Neuroimage* 62, 774-781.

803 Fischl, B., Dale, A.M., 2000. Measuring the thickness of the human cerebral cortex from magnetic
804 resonance images. *Proc Natl Acad Sci U S A* 97, 11050-11055.

805 Fortin, J.P., Cullen, N., Sheline, Y.I., Taylor, W.D., Aselcioglu, I., Cook, P.A., Adams, P., Cooper, C.,
806 Fava, M., McGrath, P.J., McInnis, M., Phillips, M.L., Trivedi, M.H., Weissman, M.M., Shinohara,
807 R.T., 2018. Harmonization of cortical thickness measurements across scanners and sites. *Neuroimage*
808 167, 104-120.

809 Fortin, J.P., Parker, D., Tunc, B., Watanabe, T., Elliott, M.A., Ruparel, K., Roalf, D.R., Satterthwaite,
810 T.D., Gur, R.C., Gur, R.E., Schultz, R.T., Verma, R., Shinohara, R.T., 2017. Harmonization of multi-
811 site diffusion tensor imaging data. *Neuroimage* 161, 149-170.

812 Fukutomi, H., Glasser, M.F., Zhang, H., Autio, J.A., Coalson, T.S., Okada, T., Togashi, K., Van Essen,
813 D.C., Hayashi, T., 2018. Neurite imaging reveals microstructural variations in human cerebral cortical
814 gray matter. *Neuroimage* 182, 488-499.

815 Glasser, M.F., Coalson, T.S., Robinson, E.C., Hacker, C.D., Harwell, J., Yacoub, E., Ugurbil, K.,
816 Andersson, J., Beckmann, C.F., Jenkinson, M., Smith, S.M., Van Essen, D.C., 2016a. A multi-modal
817 parcellation of human cerebral cortex. *Nature* 536, 171-178.

818 Glasser, M.F., Smith, S.M., Marcus, D.S., Andersson, J.L., Auerbach, E.J., Behrens, T.E., Coalson, T.S.,
819 Harms, M.P., Jenkinson, M., Moeller, S., Robinson, E.C., Sotiropoulos, S.N., Xu, J., Yacoub, E.,
820 Ugurbil, K., Van Essen, D.C., 2016b. The Human Connectome Project's neuroimaging approach. *Nat*
821 *Neurosci* 19, 1175-1187.

822 Glasser, M.F., Sotiropoulos, S.N., Wilson, J.A., Coalson, T.S., Fischl, B., Andersson, J.L., Xu, J., Jbabdi,
823 S., Webster, M., Polimeni, J.R., Van Essen, D.C., Jenkinson, M., Consortium, W.U.-M.H., 2013. The
824 minimal preprocessing pipelines for the Human Connectome Project. *Neuroimage* 80, 105-124.

825 Glasser, M.F., Van Essen, D.C., 2011. Mapping human cortical areas in vivo based on myelin content as
826 revealed by T1- and T2-weighted MRI. *J Neurosci* 31, 11597-11616.

827 Harms, M.P., Somerville, L.H., Ances, B.M., Andersson, J., Barch, D.M., Bastiani, M., Bookheimer,
828 S.Y., Brown, T.B., Buckner, R.L., Burgess, G.C., Coalson, T.S., Chappell, M.A., Dapretto, M.,
829 Douaud, G., Fischl, B., Glasser, M.F., Greve, D.N., Hodge, C., Jamison, K.W., Jbabdi, S., Kandala, S.,
830 Li, X., Mair, R.W., Mangia, S., Marcus, D., Mascali, D., Moeller, S., Nichols, T.E., Robinson, E.C.,
831 Salat, D.H., Smith, S.M., Sotiropoulos, S.N., Terpstra, M., Thomas, K.M., Tisdall, M.D., Ugurbil, K.,
832 van der Kouwe, A., Woods, R.P., Zollei, L., Van Essen, D.C., Yacoub, E., 2018. Extending the
833 Human Connectome Project across ages: Imaging protocols for the Lifespan Development and Aging
834 projects. *Neuroimage* 183, 972-984.

835 Hibar, D.P., Westlye, L.T., Doan, N.T., Jahanshad, N., Cheung, J.W., Ching, C.R.K., Versace, A.,
836 Bilderbeck, A.C., Uhlmann, A., Mwangi, B., Kramer, B., Overs, B., Hartberg, C.B., Abe, C., Dima,
837 D., Grotegerd, D., Sprooten, E., Boen, E., Jimenez, E., Howells, F.M., Delvecchio, G., Temmingh, H.,
838 Starke, J., Almeida, J.R.C., Goikolea, J.M., Houenou, J., Beard, L.M., Rauer, L., Abramovic, L.,
839 Bonnin, M., Ponteduro, M.F., Keil, M., Rive, M.M., Yao, N., Yalin, N., Najt, P., Rosa, P.G., Redlich,
840 R., Trost, S., Hagenaars, S., Fears, S.C., Alonso-Lana, S., van Erp, T.G.M., Nickson, T., Chaim-
841 Avancini, T.M., Meier, T.B., Elvsashagen, T., Haukvik, U.K., Lee, W.H., Schene, A.H., Lloyd, A.J.,
842 Young, A.H., Nugent, A., Dale, A.M., Pfenning, A., McIntosh, A.M., Lafer, B., Baune, B.T., Ekman,
843 C.J., Zarate, C.A., Bearden, C.E., Henry, C., Simhandl, C., McDonald, C., Bourne, C., Stein, D.J.,
844 Wolf, D.H., Cannon, D.M., Glahn, D.C., Veltman, D.J., Pomarol-Clotet, E., Vieta, E., Canales-
845 Rodriguez, E.J., Nery, F.G., Duran, F.L.S., Busatto, G.F., Roberts, G., Pearlson, G.D., Goodwin,

- 846 G.M., Kugel, H., Whalley, H.C., Ruhe, H.G., Soares, J.C., Fullerton, J.M., Rybakowski, J.K., Savitz,
847 J., Chaim, K.T., Fatjo-Vilas, M., Soeiro-de-Souza, M.G., Boks, M.P., Zanetti, M.V., Otaduy, M.C.G.,
848 Schaufelberger, M.S., Alda, M., Ingvar, M., Phillips, M.L., Kempton, M.J., Bauer, M., Landen, M.,
849 Lawrence, N.S., van Haren, N.E.M., Horn, N.R., Freimer, N.B., Gruber, O., Schofield, P.R., Mitchell,
850 P.B., Kahn, R.S., Lenroot, R., Machado-Vieira, R., Ophoff, R.A., Sarro, S., Frangou, S., Satterthwaite,
851 T.D., Hajek, T., Dannlowski, U., Malt, U.F., Arolt, V., Gattaz, W.F., Drevets, W.C., Caseras, X.,
852 Agartz, I., Thompson, P.M., Andreassen, O.A., 2018. Cortical abnormalities in bipolar disorder: an
853 MRI analysis of 6503 individuals from the ENIGMA Bipolar Disorder Working Group. *Mol*
854 *Psychiatry* 23, 932-942.
- 855 Iwatsubo, T., Iwata, A., Suzuki, K., Ihara, R., Arai, H., Ishii, K., Senda, M., Ito, K., Ikeuchi, T., Kuwano,
856 R., Matsuda, H., Japanese Alzheimer's Disease Neuroimaging, I., Sun, C.K., Beckett, L.A., Petersen,
857 R.C., Weiner, M.W., Aisen, P.S., Donohue, M.C., Alzheimer's Disease Neuroimaging, I., 2018.
858 Japanese and North American Alzheimer's Disease Neuroimaging Initiative studies: Harmonization
859 for international trials. *Alzheimers Dement* 14, 1077-1087.
- 860 Koike, S., Takano, Y., Iwashiro, N., Satomura, Y., Suga, M., Nagai, T., Natsubori, T., Tada, M.,
861 Nishimura, Y., Yamasaki, S., Takizawa, R., Yahata, N., Araki, T., Yamasue, H., Kasai, K., 2013. A
862 multimodal approach to investigate biomarkers for psychosis in a clinical setting: the Integrative
863 Neuroimaging studies in Schizophrenia Targeting for Early intervention and Prevention (IN-STEP)
864 project *Schizophr Res* 143, 116-124.
- 865 Koutsouleris, N., Meisenzahl, E.M., Borgwardt, S., Riecher-Rössler, A., Frodl, T., Kambitz, J., Kohler,
866 Y., Falkai, P., Moller, H.J., Reiser, M., Davatzikos, C., 2015. Individualized differential diagnosis of
867 schizophrenia and mood disorders using neuroanatomical biomarkers. *Brain* 138, 2059-2073.
- 868 Lee, T.Y., Kwon, J.S., 2016. Psychosis research in Asia: advantage from low prevalence of cannabis use.
869 *NPJ Schizophr* 2, 1.
- 870 Marcus, D.S., Harms, M.P., Snyder, A.Z., Jenkinson, M., Wilson, J.A., Glasser, M.F., Barch, D.M.,
871 Archie, K.A., Burgess, G.C., Ramaratnam, M., Hodge, M., Horton, W., Herrick, R., Olsen, T.,
872 McKay, M., House, M., Hileman, M., Reid, E., Harwell, J., Coalson, T., Schindler, J., Elam, J.S.,
873 Curtiss, S.W., Van Essen, D.C., Consortium, W.U.-M.H., 2013. Human Connectome Project
874 informatics: quality control, database services, and data visualization. *Neuroimage* 80, 202-219.
- 875 Miller, K.L., Alfaro-Almagro, F., Bangerter, N.K., Thomas, D.L., Yacoub, E., Xu, J., Bartsch, A.J.,
876 Jbabdi, S., Sotiropoulos, S.N., Andersson, J.L., Griffanti, L., Douaud, G., Okell, T.W., Weale, P.,
877 Dragonu, I., Garratt, S., Hudson, S., Collins, R., Jenkinson, M., Matthews, P.M., Smith, S.M., 2016.
878 Multimodal population brain imaging in the UK Biobank prospective epidemiological study. *Nat*
879 *Neurosci* 19, 1523-1536.
- 880 Moeller, S., Yacoub, E., Olfman, C.A., Auerbach, E., Strupp, J., Harel, N., Ugurbil, K., 2010. Multiband
881 multislice GE-EPI at 7 tesla, with 16-fold acceleration using partial parallel imaging with application
882 to high spatial and temporal whole-brain fMRI. *Magn Reson Med* 63, 1144-1153.
- 883 Mueller, S.G., Weiner, M.W., Thal, L.J., Petersen, R.C., Jack, C., Jagust, W., Trojanowski, J.Q., Toga,
884 A.W., Beckett, L., 2005. The Alzheimer's disease neuroimaging initiative. *Neuroimaging Clin N Am*
885 15, 869-877, xi-xii.
- 886 Mukai, Y., Murata, M., 2017. Japan Parkinson's Progression Markers Initiative (J-PPMI). *Nihon Rinsho*
887 75, 151-155.
- 888 Murray, C.J., Vos, T., Lozano, R., Naghavi, M., Flaxman, A.D., Michaud, C., Ezzati, M., Shibuya, K.,
889 Salomon, J.A., Abdalla, S., Aboyans, V., Abraham, J., Ackerman, I., Aggarwal, R., Ahn, S.Y., Ali,
890 M.K., Alvarado, M., Anderson, H.R., Anderson, L.M., Andrews, K.G., Atkinson, C., Baddour, L.M.,
891 Bahalim, A.N., Barker-Collo, S., Barrero, L.H., Bartels, D.H., Basanez, M.G., Baxter, A., Bell, M.L.,
892 Benjamin, E.J., Bennett, D., Bernabe, E., Bhalla, K., Bhandari, B., Bikbov, B., Bin Abdulhak, A.,
893 Birbeck, G., Black, J.A., Blencowe, H., Blore, J.D., Blyth, F., Bolliger, I., Bonaventure, A., Boufous,
894 S., Bourne, R., Boussinesq, M., Braithwaite, T., Brayne, C., Bridgett, L., Brooker, S., Brooks, P.,
895 Brugha, T.S., Bryan-Hancock, C., Bucello, C., Buchbinder, R., Buckle, G., Budke, C.M., Burch, M.,
896 Burney, P., Burstein, R., Calabria, B., Campbell, B., Canter, C.E., Carabin, H., Carapetis, J., Carmona,

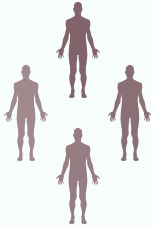
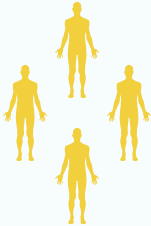
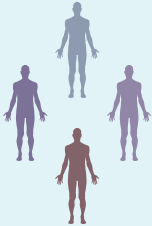
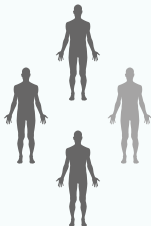
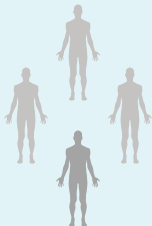
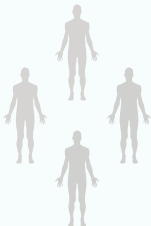
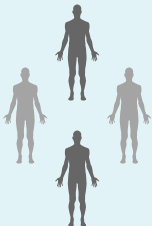




897 L., Cella, C., Charlson, F., Chen, H., Cheng, A.T., Chou, D., Chugh, S.S., Coffeng, L.E., Colan, S.D.,
898 Colquhoun, S., Colson, K.E., Condon, J., Connor, M.D., Cooper, L.T., Corriere, M., Cortinovis, M.,
899 de Vaccaro, K.C., Couser, W., Cowie, B.C., Criqui, M.H., Cross, M., Dabhadkar, K.C., Dahiya, M.,
900 Dahodwala, N., Damsere-Derry, J., Danaei, G., Davis, A., De Leo, D., Degenhardt, L., Dellavalle, R.,
901 Delossantos, A., Denenberg, J., Derrett, S., Des Jarlais, D.C., Dharmaratne, S.D., Dherani, M., Diaz-
902 Torne, C., Dolk, H., Dorsey, E.R., Driscoll, T., Duber, H., Ebel, B., Edmond, K., Elbaz, A., Ali, S.E.,
903 Erskine, H., Erwin, P.J., Espindola, P., Ewoigbokhan, S.E., Farzadfar, F., Feigin, V., Felson, D.T.,
904 Ferrari, A., Ferri, C.P., Fevre, E.M., Finucane, M.M., Flaxman, S., Flood, L., Foreman, K.,
905 Forouzanfar, M.H., Fowkes, F.G., Fransen, M., Freeman, M.K., Gabbe, B.J., Gabriel, S.E., Gakidou,
906 E., Ganatra, H.A., Garcia, B., Gaspari, F., Gillum, R.F., Gmel, G., Gonzalez-Medina, D., Gosselin, R.,
907 Grainger, R., Grant, B., Groeger, J., Guillemin, F., Gunnell, D., Gupta, R., Haagsma, J., Hagan, H.,
908 Halasa, Y.A., Hall, W., Haring, D., Haro, J.M., Harrison, J.E., Havmoeller, R., Hay, R.J., Higashi, H.,
909 Hill, C., Hoen, B., Hoffman, H., Hotez, P.J., Hoy, D., Huang, J.J., Ibeanusi, S.E., Jacobsen, K.H.,
910 James, S.L., Jarvis, D., Jirasaria, R., Jayaraman, S., Johns, N., Jonas, J.B., Karthikeyan, G.,
911 Kassebaum, N., Kawakami, N., Keren, A., Khoo, J.P., King, C.H., Knowlton, L.M., Kobusingye, O.,
912 Koranteng, A., Krishnamurthi, R., Laden, F., Laloo, R., Laslett, L.L., Lathlean, T., Leasher, J.L., Lee,
913 Y.Y., Leigh, J., Levinson, D., Lim, S.S., Limb, E., Lin, J.K., Lipnick, M., Lipshultz, S.E., Liu, W.,
914 Loane, M., Ohno, S.L., Lyons, R., Mabweijano, J., MacIntyre, M.F., Malekzadeh, R., Mallinger, L.,
915 Manivannan, S., Marcenes, W., March, L., Margolis, D.J., Marks, G.B., Marks, R., Matsumori, A.,
916 Matzopoulos, R., Mayosi, B.M., McAnulty, J.H., McDermott, M.M., McGill, N., McGrath, J.,
917 Medina-Mora, M.E., Meltzer, M., Mensah, G.A., Merriman, T.R., Meyer, A.C., Miglioli, V., Miller,
918 M., Miller, T.R., Mitchell, P.B., Mock, C., Mocumbi, A.O., Moffitt, T.E., Mokdad, A.A., Monasta, L.,
919 Montico, M., Moradi-Lakeh, M., Moran, A., Morawska, L., Mori, R., Murdoch, M.E., Mwaniki, M.K.,
920 Naidoo, K., Nair, M.N., Naldi, L., Narayan, K.M., Nelson, P.K., Nelson, R.G., Nevitt, M.C., Newton,
921 C.R., Nolte, S., Norman, P., Norman, R., O'Donnell, M., O'Hanlon, S., Olives, C., Omer, S.B.,
922 Ortblad, K., Osborne, R., Ozgediz, D., Page, A., Pahari, B., Pandian, J.D., Rivero, A.P., Patten, S.B.,
923 Pearce, N., Padilla, R.P., Perez-Ruiz, F., Perico, N., Pesudovs, K., Phillips, D., Phillips, M.R., Pierce,
924 K., Pion, S., Polanczyk, G.V., Polinder, S., Pope, C.A., 3rd, Popova, S., Porrini, E., Pourmalek, F.,
925 Prince, M., Pullan, R.L., Ramaiah, K.D., Ranganathan, D., Razavi, H., Regan, M., Rehm, J.T., Rein,
926 D.B., Remuzzi, G., Richardson, K., Rivara, F.P., Roberts, T., Robinson, C., De Leon, F.R., Ronfani,
927 L., Room, R., Rosenfeld, L.C., Rushton, L., Sacco, R.L., Saha, S., Sampson, U., Sanchez-Riera, L.,
928 Sanman, E., Schwebel, D.C., Scott, J.G., Segui-Gomez, M., Shahraz, S., Shepard, D.S., Shin, H.,
929 Shivakoti, R., Singh, D., Singh, G.M., Singh, J.A., Singleton, J., Sleet, D.A., Sliwa, K., Smith, E.,
930 Smith, J.L., Stapelberg, N.J., Steer, A., Steiner, T., Stolk, W.A., Stovner, L.J., Sudfeld, C., Syed, S.,
931 Tamburlini, G., Tavakkoli, M., Taylor, H.R., Taylor, J.A., Taylor, W.J., Thomas, B., Thomson, W.M.,
932 Thurston, G.D., Tleyjeh, I.M., Tonelli, M., Towbin, J.A., Truelsen, T., Tsilimbaris, M.K., Ubeda, C.,
933 Undurraga, E.A., van der Werf, M.J., van Os, J., Vavilala, M.S., Venketasubramanian, N., Wang, M.,
934 Wang, W., Watt, K., Weatherall, D.J., Weinstock, M.A., Weintraub, R., Weisskopf, M.G., Weissman,
935 M.M., White, R.A., Whiteford, H., Wiebe, N., Wiersma, S.T., Wilkinson, J.D., Williams, H.C.,
936 Williams, S.R., Witt, E., Wolfe, F., Woolf, A.D., Wulf, S., Yeh, P.H., Zaidi, A.K., Zheng, Z.J., Zonies,
937 D., Lopez, A.D., AlMazroa, M.A., Memish, Z.A., 2012. Disability-adjusted life years (DALYs) for
938 291 diseases and injuries in 21 regions, 1990-2010: a systematic analysis for the Global Burden of
939 Disease Study 2010. *Lancet* 380, 2197-2223.

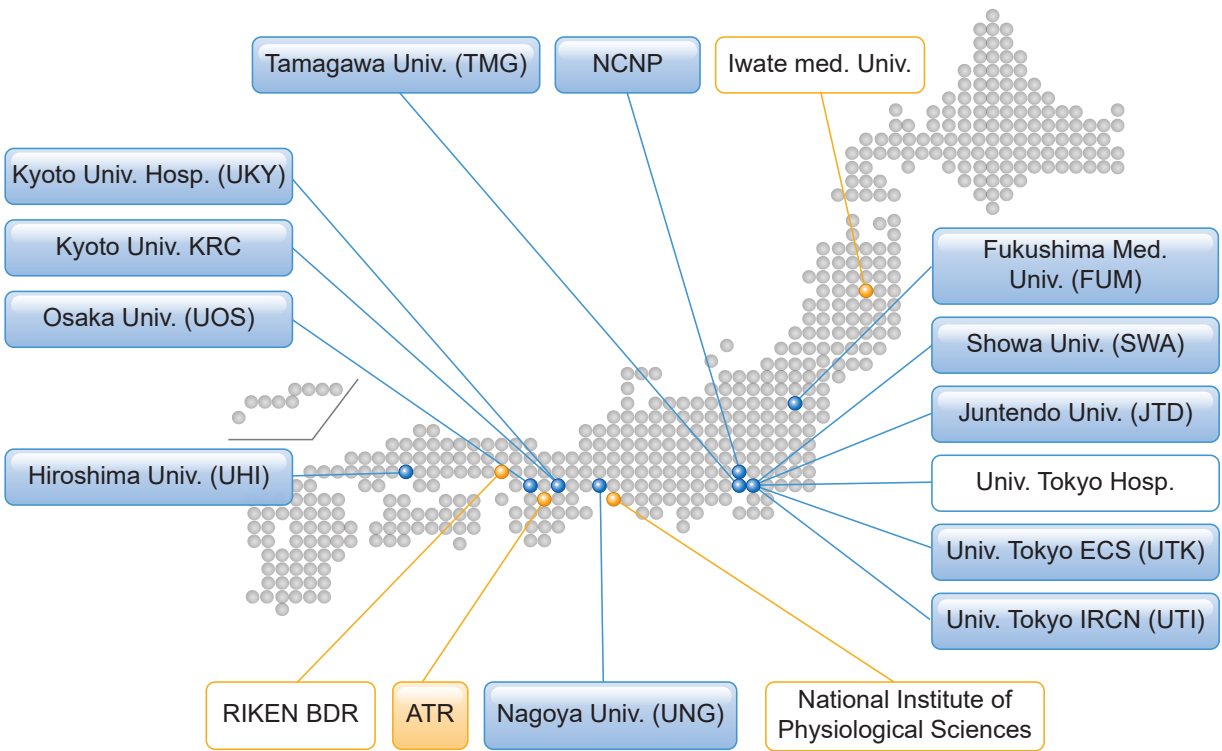
940 Nunes, A., Schnack, H.G., Ching, C.R.K., Agartz, I., Akudjedu, T.N., Alda, M., Alnaes, D., Alonso-Lana,
941 S., Bauer, J., Baune, B.T., Boen, E., Bonnin, C.D.M., Busatto, G.F., Canales-Rodriguez, E.J., Cannon,
942 D.M., Caseras, X., Chaim-Avancini, T.M., Dannlowski, U., Diaz-Zuluaga, A.M., Dietsche, B., Doan,
943 N.T., Duchesnay, E., Elvsashagen, T., Emden, D., Eyler, L.T., Fatjo-Vilas, M., Favre, P., Foley, S.F.,
944 Fullerton, J.M., Glahn, D.C., Goikolea, J.M., Grotegerd, D., Hahn, T., Henry, C., Hibar, D.P.,
945 Houenou, J., Howells, F.M., Jahanshad, N., Kaufmann, T., Kenney, J., Kircher, T.T.J., Krug, A.,
946 Lagerberg, T.V., Lenroot, R.K., Lopez-Jaramillo, C., Machado-Vieira, R., Malt, U.F., McDonald, C.,
947 Mitchell, P.B., Mwangi, B., Nabulsi, L., Opel, N., Overs, B.J., Pineda-Zapata, J.A., Pomarol-Clotet,

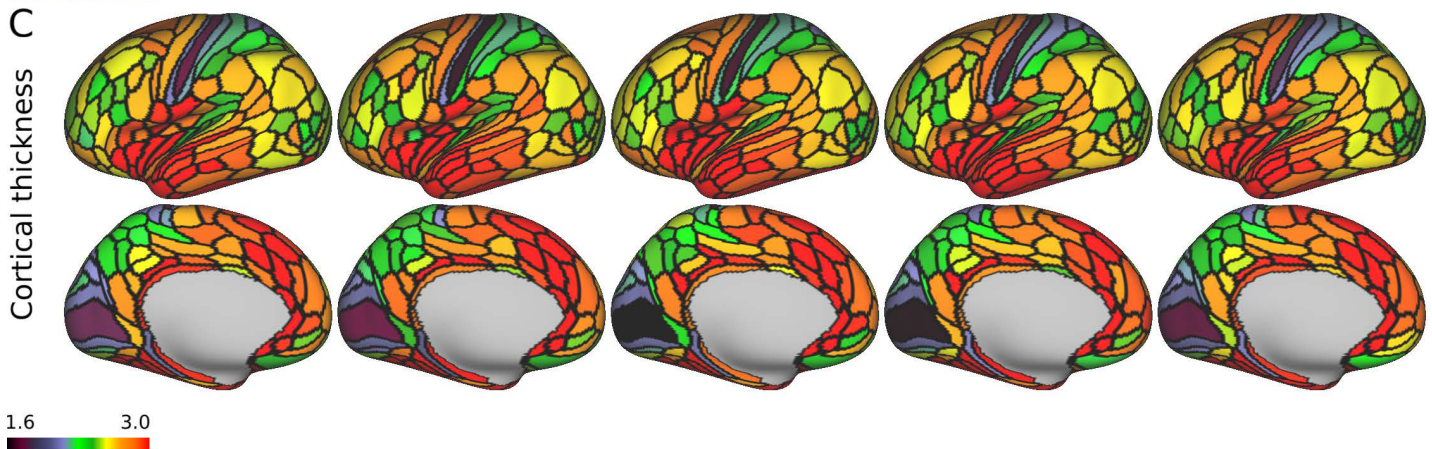
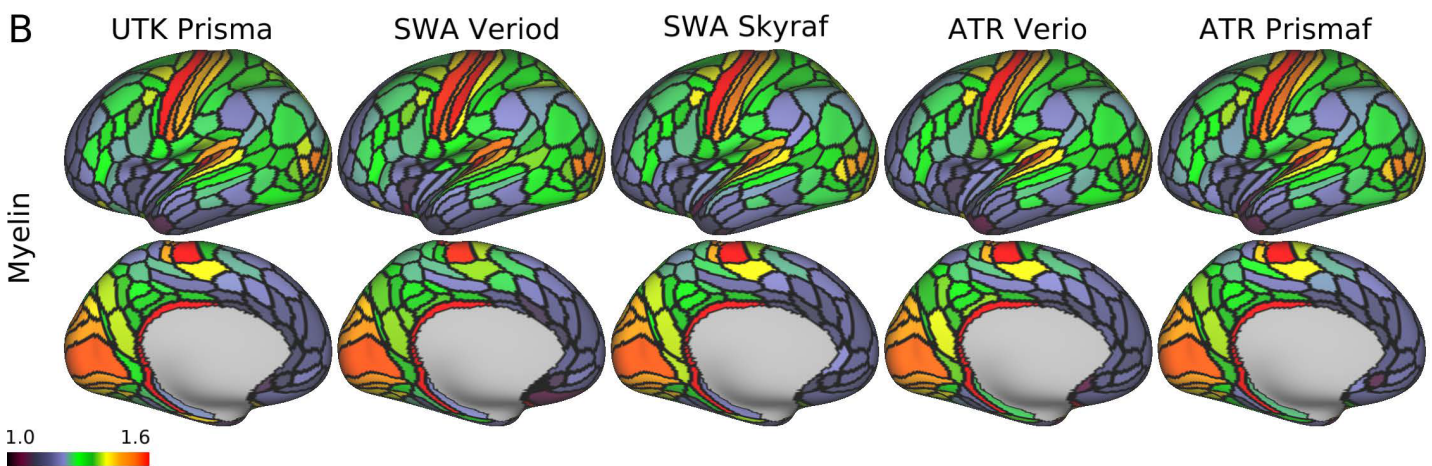
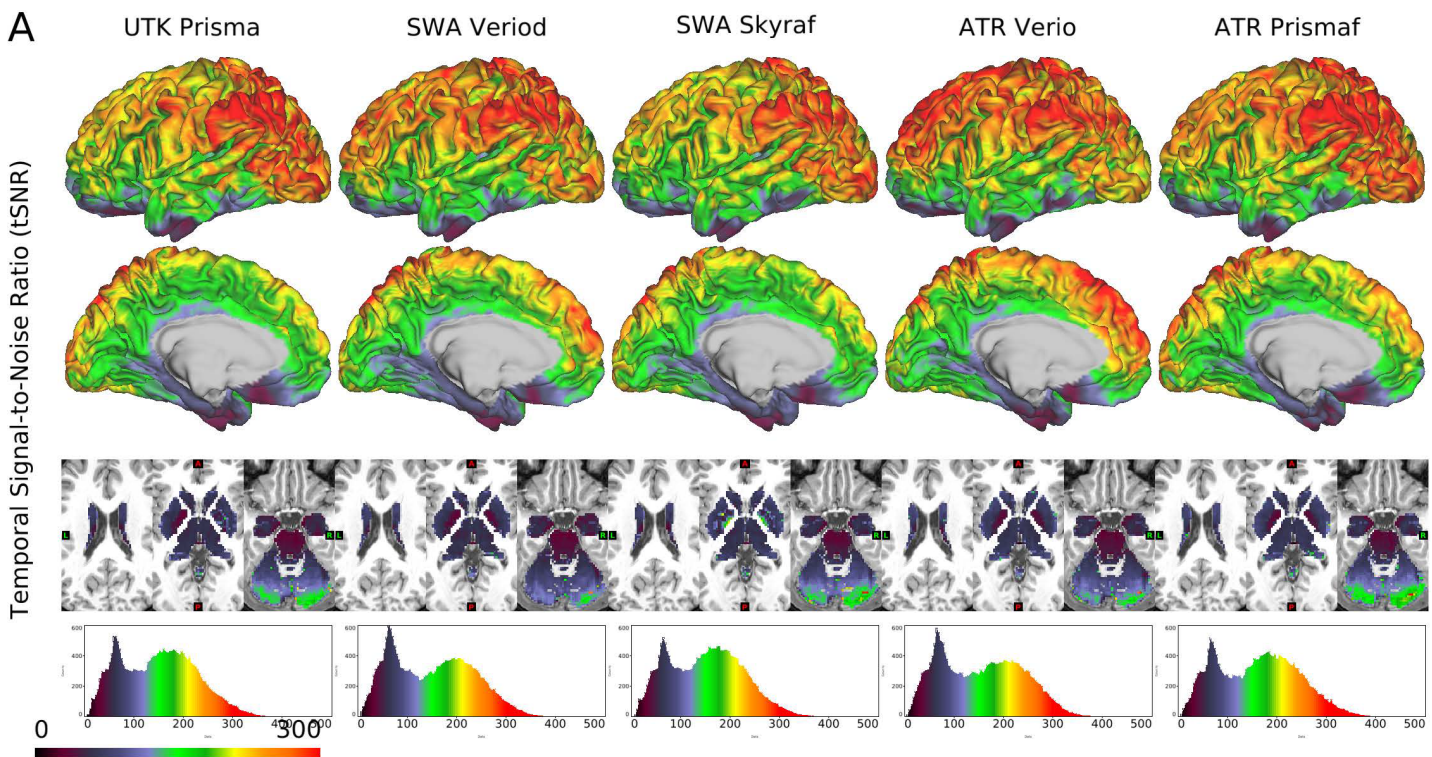
- 948 E., Redlich, R., Roberts, G., Rosa, P.G., Salvador, R., Satterthwaite, T.D., Soares, J.C., Stein, D.J.,
949 Temmingh, H.S., Trappenberg, T., Uhlmann, A., van Haren, N.E.M., Vieta, E., Westlye, L.T., Wolf,
950 D.H., Yuksel, D., Zanetti, M.V., Andreassen, O.A., Thompson, P.M., Hajek, T., Group, E.B.D.W.,
951 2018. Using structural MRI to identify bipolar disorders - 13 site machine learning study in 3020
952 individuals from the ENIGMA Bipolar Disorders Working Group. *Mol Psychiatry*.
- 953 O'Shea, A., Cohen, R.A., Porges, E.C., Nissim, N.R., Woods, A.J., 2016. Cognitive Aging and the
954 Hippocampus in Older Adults. *Front Aging Neurosci* 8, 298.
- 955 Okada, N., Ando, S., Sanada, M., Hirata-Mogi, S., Iijima, Y., Sugiyama, H., Shirakawa, T., Yamagishi,
956 M., Kanehara, A., Morita, M., Yagi, T., Hayashi, N., Koshiyama, D., Morita, K., Sawada, K.,
957 Ikegame, T., Sugimoto, N., Toriyama, R., Masaoka, M., Fujikawa, S., Kanata, S., Tada, M., Kirihara,
958 K., Yahata, N., Araki, T., Jinde, S., Kano, Y., Koike, S., Endo, K., Yamasaki, S., Nishida, A., Hiraiwa-
959 Hasegawa, M., Bundo, M., Iwamoto, K., Tanaka, S.C., Kasai, K., 2019. Population-neuroscience
960 study of the Tokyo TEEN Cohort (pn-TTC): Cohort longitudinal study to explore the neurobiological
961 substrates of adolescent psychological and behavioral development. *Psychiatry Clin Neurosci* 73, 231-
962 242.
- 963 Okada, N., Fukunaga, M., Yamashita, F., Koshiyama, D., Yamamori, H., Ohi, K., Yasuda, Y., Fujimoto,
964 M., Watanabe, Y., Yahata, N., Nemoto, K., Hibar, D.P., van Erp, T.G., Fujino, H., Isobe, M., Isomura,
965 S., Natsubori, T., Narita, H., Hashimoto, N., Miyata, J., Koike, S., Takahashi, T., Yamasue, H.,
966 Matsuo, K., Onitsuka, T., Iidaka, T., Kawasaki, Y., Yoshimura, R., Watanabe, Y., Suzuki, M., Turner,
967 J.A., Takeda, M., Thompson, P.M., Ozaki, N., Kasai, K., Hashimoto, R., 2016. Abnormal asymmetries
968 in subcortical brain volume in schizophrenia. *Mol Psychiatry* 21, 1460-1466.
- 969 Parkinson Progression Marker Initiative, 2011. The Parkinson Progression Marker Initiative (PPMI). *Prog*
970 *Neurobiol* 95, 629-635.
- 971 R Core Team, 2018. R: A language and environment for statistical computing. R Foundation for
972 Statistical Computing. Vienna, Austria.
- 973 Robinson, E.C., Garcia, K., Glasser, M.F., Chen, Z., Coalson, T.S., Makropoulos, A., Bozek, J., Wright,
974 R., Schuh, A., Webster, M., Hutter, J., Price, A., Cordero Grande, L., Hughes, E., Tusor, N., Bayly,
975 P.V., Van Essen, D.C., Smith, S.M., Edwards, A.D., Hajnal, J., Jenkinson, M., Glocker, B., Rueckert,
976 D., 2018. Multimodal surface matching with higher-order smoothness constraints. *Neuroimage* 167,
977 453-465.
- 978 Sadato, N., Morita, K., Kasai, K., Fukushi, T., Nakamura, K., Nakazawa, E., Okano, H., Okabe, S., 2019.
979 Neuroethical Issues of the Brain/MINDS Project of Japan. *Neuron* 101, 385-389.
- 980 Salimi-Khorshidi, G., Douaud, G., Beckmann, C.F., Glasser, M.F., Griffanti, L., Smith, S.M., 2014.
981 Automatic denoising of functional MRI data: combining independent component analysis and
982 hierarchical fusion of classifiers. *Neuroimage* 90, 449-468.
- 983 Schmaal, L., Hibar, D.P., Samann, P.G., Hall, G.B., Baune, B.T., Jahanshad, N., Cheung, J.W., van Erp,
984 T.G.M., Bos, D., Ikram, M.A., Vernooij, M.W., Niessen, W.J., Tiemeier, H., Hofman, A., Wittfeld,
985 K., Grabe, H.J., Janowitz, D., Bulow, R., Selonke, M., Volzke, H., Grottegerd, D., Dannlowski, U.,
986 Arolt, V., Opel, N., Heindel, W., Kugel, H., Hoehn, D., Czisch, M., Couvy-Duchesne, B., Renteria,
987 M.E., Strike, L.T., Wright, M.J., Mills, N.T., de Zubicaray, G.I., McMahon, K.L., Medland, S.E.,
988 Martin, N.G., Gillespie, N.A., Goya-Maldonado, R., Gruber, O., Kramer, B., Hatton, S.N.,
989 Lagopoulos, J., Hickie, I.B., Frodl, T., Carballedo, A., Frey, E.M., van Velzen, L.S., Penninx, B., van
990 Tol, M.J., van der Wee, N.J., Davey, C.G., Harrison, B.J., Mwangi, B., Cao, B., Soares, J.C., Veer,
991 I.M., Walter, H., Schoepf, D., Zurovski, B., Konrad, C., Schramm, E., Normann, C., Schnell, K.,
992 Sacchet, M.D., Gotlib, I.H., MacQueen, G.M., Godlewska, B.R., Nickson, T., McIntosh, A.M.,
993 Pampmeyer, M., Whalley, H.C., Hall, J., Sussmann, J.E., Li, M., Walter, M., Aftanas, L., Brack, I.,
994 Bokhan, N.A., Thompson, P.M., Veltman, D.J., 2017. Cortical abnormalities in adults and adolescents
995 with major depression based on brain scans from 20 cohorts worldwide in the ENIGMA Major
996 Depressive Disorder Working Group. *Mol Psychiatry* 22, 900-909.
- 997 Schmaal, L., Veltman, D.J., van Erp, T.G., Samann, P.G., Frodl, T., Jahanshad, N., Loehrer, E., Tiemeier,
998 H., Hofman, A., Niessen, W.J., Vernooij, M.W., Ikram, M.A., Wittfeld, K., Grabe, H.J., Block, A.,

- 999 Hegenscheid, K., Volzke, H., Hoehn, D., Czisch, M., Lagopoulos, J., Hatton, S.N., Hickie, I.B., Goya-
1000 Maldonado, R., Kramer, B., Gruber, O., Couvy-Duchesne, B., Renteria, M.E., Strike, L.T., Mills,
1001 N.T., de Zubicaray, G.I., McMahon, K.L., Medland, S.E., Martin, N.G., Gillespie, N.A., Wright, M.J.,
1002 Hall, G.B., MacQueen, G.M., Frey, E.M., Carballo, A., van Velzen, L.S., van Tol, M.J., van der
1003 Wee, N.J., Veer, I.M., Walter, H., Schnell, K., Schramm, E., Normann, C., Schoepf, D., Konrad, C.,
1004 Zurowski, B., Nickson, T., McIntosh, A.M., Pappmeyer, M., Whalley, H.C., Sussmann, J.E.,
1005 Godlewska, B.R., Cowen, P.J., Fischer, F.H., Rose, M., Penninx, B.W., Thompson, P.M., Hibar, D.P.,
1006 2016. Subcortical brain alterations in major depressive disorder: findings from the ENIGMA Major
1007 Depressive Disorder working group. *Mol Psychiatry* 21, 806-812.
- 1008 Setsompop, K., Gagoski, B.A., Polimeni, J.R., Witzel, T., Wedeen, V.J., Wald, L.L., 2012. Blipped-
1009 controlled aliasing in parallel imaging for simultaneous multislice echo planar imaging with reduced
1010 g-factor penalty. *Magn Reson Med* 67, 1210-1224.
- 1011 Smith, S.M., Nichols, T.E., Vidaurre, D., Winkler, A.M., Behrens, T.E., Glasser, M.F., Ugurbil, K.,
1012 Barch, D.M., Van Essen, D.C., Miller, K.L., 2015. A positive-negative mode of population covariation
1013 links brain connectivity, demographics and behavior. *Nat Neurosci* 18, 1565-1567.
- 1014 Somerville, L.H., Bookheimer, S.Y., Buckner, R.L., Burgess, G.C., Curtiss, S.W., Dapretto, M., Elam,
1015 J.S., Gaffrey, M.S., Harms, M.P., Hodge, C., Kandala, S., Kastman, E.K., Nichols, T.E., Schlaggar,
1016 B.L., Smith, S.M., Thomas, K.M., Yacoub, E., Van Essen, D.C., Barch, D.M., 2018. The Lifespan
1017 Human Connectome Project in Development: A large-scale study of brain connectivity development
1018 in 5-21 year olds. *Neuroimage* 183, 456-468.
- 1019 Sotiropoulos, S.N., Hernandez-Fernandez, M., Vu, A.T., Andersson, J.L., Moeller, S., Yacoub, E.,
1020 Lenglet, C., Ugurbil, K., Behrens, T.E.J., Jbabdi, S., 2016. Fusion in diffusion MRI for improved fibre
1021 orientation estimation: An application to the 3T and 7T data of the Human Connectome Project.
1022 *Neuroimage* 134, 396-409.
- 1023 van Erp, T.G., Hibar, D.P., Rasmussen, J.M., Glahn, D.C., Pearlson, G.D., Andreassen, O.A., Agartz, I.,
1024 Westlye, L.T., Haukvik, U.K., Dale, A.M., Melle, I., Hartberg, C.B., Gruber, O., Kraemer, B., Zilles,
1025 D., Donohoe, G., Kelly, S., McDonald, C., Morris, D.W., Cannon, D.M., Corvin, A., Machielsen,
1026 M.W., Koenders, L., de Haan, L., Veltman, D.J., Satterthwaite, T.D., Wolf, D.H., Gur, R.C., Gur,
1027 R.E., Potkin, S.G., Mathalon, D.H., Mueller, B.A., Preda, A., Macciardi, F., Ehrlich, S., Walton, E.,
1028 Hass, J., Calhoun, V.D., Bockholt, H.J., Sponheim, S.R., Shoemaker, J.M., van Haren, N.E., Hulshoff
1029 Pol, H.E., Ophoff, R.A., Kahn, R.S., Roiz-Santianez, R., Crespo-Facorro, B., Wang, L., Alpert, K.I.,
1030 Jonsson, E.G., Dimitrova, R., Bois, C., Whalley, H.C., McIntosh, A.M., Lawrie, S.M., Hashimoto, R.,
1031 Thompson, P.M., Turner, J.A., 2016. Subcortical brain volume abnormalities in 2028 individuals with
1032 schizophrenia and 2540 healthy controls via the ENIGMA consortium. *Mol Psychiatry* 21, 547-553.
- 1033 Van Essen, D.C., Ugurbil, K., Auerbach, E., Barch, D., Behrens, T.E., Bucholz, R., Chang, A., Chen, L.,
1034 Corbetta, M., Curtiss, S.W., Della Penna, S., Feinberg, D., Glasser, M.F., Harel, N., Heath, A.C.,
1035 Larson-Prior, L., Marcus, D., Michalareas, G., Moeller, S., Oostenveld, R., Petersen, S.E., Prior, F.,
1036 Schlaggar, B.L., Smith, S.M., Snyder, A.Z., Xu, J., Yacoub, E., Consortium, W.U.-M.H., 2012. The
1037 Human Connectome Project: a data acquisition perspective. *Neuroimage* 62, 2222-2231.
- 1038 Wang, Y., Xu, Q., Luo, J., Hu, M., Zuo, C., 2019. Effects of Age and Sex on Subcortical Volumes. *Front*
1039 *Aging Neurosci* 11, 259.
- 1040 Weiner, M.W., Veitch, D.P., Aisen, P.S., Beckett, L.A., Cairns, N.J., Cedarbaum, J., Green, R.C., Harvey,
1041 D., Jack, C.R., Jagust, W., Luthman, J., Morris, J.C., Petersen, R.C., Saykin, A.J., Shaw, L., Shen, L.,
1042 Schwarz, A., Toga, A.W., Trojanowski, J.Q., Alzheimer's Disease Neuroimaging, I., 2015. 2014
1043 Update of the Alzheimer's Disease Neuroimaging Initiative: A review of papers published since its
1044 inception. *Alzheimers Dement* 11, e1-120.
- 1045 Winter, W., Sheridan, M., 2014. Previous reward decreases errors of commission on later 'No-Go' trials in
1046 children 4 to 12 years of age: evidence for a context monitoring account. *Dev Sci* 17, 797-807.
- 1047 Xu, J., Moeller, S., Auerbach, E.J., Strupp, J., Smith, S.M., Feinberg, D.A., Yacoub, E., Ugurbil, K.,
1048 2013. Evaluation of slice accelerations using multiband echo planar imaging at 3 T. *Neuroimage* 83,
1049 991-1001.

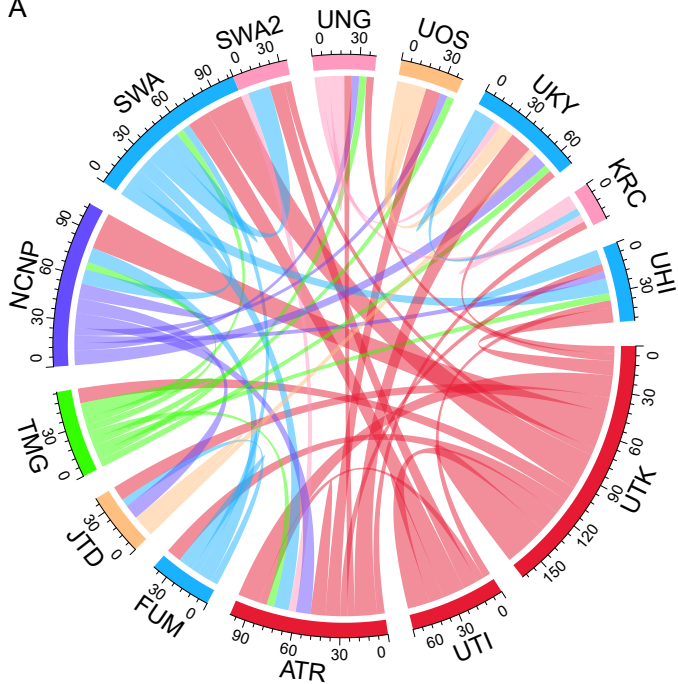
- 1050 Yahata, N., Morimoto, J., Hashimoto, R., Lisi, G., Shibata, K., Kawakubo, Y., Kuwabara, H., Kuroda,
1051 M., Yamada, T., Megumi, F., Imamizu, H., Nanez, J.E., Sr., Takahashi, H., Okamoto, Y., Kasai, K.,
1052 Kato, N., Sasaki, Y., Watanabe, T., Kawato, M., 2016. A small number of abnormal brain connections
1053 predicts adult autism spectrum disorder. *Nat Commun* 7, 11254.
- 1054 Yamashita, A., Yahata, N., Itahashi, T., Lisi, G., Yamada, T., Ichikawa, N., Takamura, M., Yoshihara, Y.,
1055 Kunimatsu, A., Okada, N., Yamagata, H., Matsuo, K., Hashimoto, R., Okada, G., Sakai, Y.,
1056 Morimoto, J., Narumoto, J., Shimada, Y., Kasai, K., Kato, N., Takahashi, H., Okamoto, Y., Tanaka,
1057 S.C., Kawato, M., Yamashita, O., Imamizu, H., 2019. Harmonization of resting-state functional MRI
1058 data across multiple imaging sites via the separation of site differences into sampling bias and
1059 measurement bias. *PLoS Biol* 17, e3000042.
- 1060 Zhang, H., Schneider, T., Wheeler-Kingshott, C.A., Alexander, D.C., 2012. NODDI: practical in vivo
1061 neurite orientation dispersion and density imaging of the human brain. *Neuroimage* 61, 1000-1016.
- 1062

Cases				
Controls (Healthy participants)				
Site Machine	Site A X	Site B X	Site C Y	Site D Z
TS 1 TS 2				





A



B

